APPROVED FOR RELEASE: 2007/02/09: CIA-RDP82-00850R000500020040-0

FOR OFFICIAL USE ONLY

JPRS L/10271

22 January 1982

Translation

RADIOPHYSICAL METHODS FOR INVESTIGATING WATER MASSES OF SNOW AND ICE

Ed. by

V.V. Bogorodskiy and V.A. Spitsyn

FBIS FOREIGN BROADCAST INFORMATION SERVICE

FOR OFFICIAL USE ONLY

APPROVED FOR RELEASE: 2007/02/09: CIA-RDP82-00850R000500020040-0

APPROVED FOR RELEASE: 2007/02/09: CIA-RDP82-00850R000500020040-0

NOTE

JPRS publications contain information primarily from foreign newspapers, periodicals and books, but also from news agency transmissions and broadcasts. Materials from foreign-language sources are translated; those from English-language sources are transcribed or reprinted, with the original phrasing and other characteristics retained.

Headlines, editorial reports, and material enclosed in brackets [] are supplied by JPRS. Processing indicators such as [Text] or [Excerpt] in the first line of each item, or following the last line of a brief, indicate how the original information was processed. Where no processing indicator is given, the information was summarized or extracted.

Unfamiliar names rendered phonetically or transliterated are enclosed in parentheses. Words or names preceded by a question mark and enclosed in parentheses were not clear in the original but have been supplied as appropriate in context. Other unattributed parenthetical notes within the body of an item originate with the source. Times within items are as given by source.

The contents of this publication in no way represent the policies, views or attitudes of the U.S. Government.

COPYRIGHT LAWS AND REGULATIONS GOVERNING OWNERSHIP OF MATERIALS REPRODUCED HEREIN REQUIRE THAT DISSEMINATION OF THIS PUBLICATION BE RESTRICTED FOR OFFICIAL USE ONLY.

APPROVED FOR RELEASE: 2007/02/09: CIA-RDP82-00850R000500020040-0

APPROVED FOR RELEASE: 2007/02/09: CIA-RDP82-00850R000500020040-0

JPRS L/10271

22 January 1982

RADIOPHYSICAL METHODS FOR INVESTIGATING WATER MASSES OF SNOW AND ICE

Leningrad TRUDY. ORDENA LENINA ARKTICHESKIY I ANTARKTICHESKIY NAUCHNO-ISSLEDOVATEL'SKIY INSTITUT. RADIOFIZICHESKIYE METODY ISSLEDOVANIY VODNYKH MASS SNEGA I L'DA in Russian No 324, 1974 pp 4-32, 50-56, 104-108, 114-117, 126-133, 144-150, 197-203

[Selected articles from collection "Radiophysical Methods for Investigating Water Masses of Snow and Ice", edited by V.V. Bogorodskiy, doctor of physical and mathematical sciences, and V.A. Spitsyn, candidate of physical and mathematical sciences, Gidrometeoizdat]

CONTENTS

APPROVED FOR RELEASE: 2007/02/09: CIA-RDP82-00850R000500020040-0

APPROVED FOR RELEASE: 2007/02/09: CIA-RDP82-00850R000500020040-0

Contents

[Text]

APPROVED FOR RELEASE: 2007/02/09: CIA-RDP82-00850R000500020040-0

APPROVED FOR RELEASE: 2007/02/09: CIA-RDP82-00850R000500020040-0

FOCUSING FACTOR IN RADIO ECHO SOUNDING OF MEDIA

Leningrad TRUDY. ORDENA LENINA ARKTICHESKIY I ANTARKTICHESKIY NAUCHNO-ISSLEDOVATEL'-SKIY INSTITUT. RADIOFIZICHESKIYE METODY ISSLEDOVANIY VODNYKH MASS SNEGA I L'DA in Russian No 324, 1974 pp 4-11

[Article by V. V. Bogorodskiy, G. V. Trepov and B. A. Fedorov]

[Text] The focusing of energy in the propagation of waves in inhomogeneous media has been repeatedly analyzed in the past [2]. However, in recently published studies on radio echo sounding of media [for example, 1, 3, 4] the focusing factor is not taken into account.

In this article the focusing factor is examined in considerable detail applicable to radio echo, slant and vertical sounding of media.

In a homogeneous medium at the distance r from a point radiation source the density of the power flux Π_0 is equal to

$$\Pi_0 = P_{rad}/4\pi r^2. \quad (1)$$

In a layered-inhomogeneous medium, where n = n(z), as a result of refraction the density of the power flux Π at this same distance is different.

The ratio

$$\eta = \frac{\Pi}{\Pi_0} \quad (2)$$

is called the focusing factor.

We will determine the focusing factor for a layered-inhomogeneous medium, in particular including here the case of wave propagation in two homogeneous media with a plane discontinuity. Assume that the radiation source is situated at the origin of coordinates (α_0 is the glancing angle of the ray at the point of emergence; α_h is the glancing angle at the observation point at the depth h; R is the horizontal range).

For an annular element dS of the area of the wave front included between the rays emerging at the angles α_0 and $\alpha_0 + d\alpha_0$, we obtain $dS = 2\pi R \sin\alpha_h dR$. Taking into account that $dR = -\partial R/\partial\alpha_0 \, d\alpha_0$ (the minus means that with h = const a greater α_0 corresponds to lesser R), we determine

APPROVED FOR RELEASE: 2007/02/09: CIA-RDP82-00850R000500020040-0

APPROVED FOR RELEASE: 2007/02/09: CIA-RDP82-00850R000500020040-0

$$dS = -2\pi R \frac{\partial R}{\partial \alpha_0} \sin \alpha_h \cdot d\alpha_0.$$

Since the power in the solid angle Ω (from α_0 to $\alpha_0 + d\alpha_0$) is equal to

[ИЗЛ = rad]

$$P_\Omega = \frac{P_{изл}}{2} \cos \alpha_0 \cdot d\alpha_0, \tag{3}$$

the density of the power flux at the distance r from the source is determined as

$$\Pi = \frac{P_{изл}}{2} \cdot \frac{\cos \alpha_0}{2\pi R \frac{\partial R}{\partial \alpha_0} \sin \alpha_h}. \tag{4}$$

Substituting expressions (1) and (4) into equation (2), we obtain an expression for the focusing factor in the following form:

$$\eta = \frac{r^2 \cos \alpha_0}{R \frac{\partial R}{\partial \alpha_0} \sin \alpha_h}. \tag{5}$$

For computing the focusing factor by the use of formula (5) it is necessary to determine R and $\partial R/\partial \alpha_0$. Taking into account that $dR = \operatorname{ctg} \alpha_z dz$, and using the Snellius law $\cos \alpha_z = 1/n(z) \cos \alpha_0$, we obtain

$$R = \int_0^h \frac{\cos \alpha_0 \, dz}{\sqrt{n(z)^2 - \cos^2 \alpha_0}}, \tag{6}$$

where α_z is the glancing angle at the depth z; n(z) is the relative refractive index of the medium at the depth z (relative to the medium at the point of emergence).

We will find the derivative $\partial R/\partial \alpha_0$ by means of differentiation of the right- and left-hand sides of expression (6) for the angle α_0

$$\frac{\partial R}{\partial \alpha_0} = \sin \alpha_0 \int_0^h \frac{n^2(z)\, dz}{[n^2(z) - \cos^2 \alpha_0]^{3/2}}. \tag{7}$$

Finally in a general case

$$\eta = \frac{r^2}{\sin \alpha_0 \sin \alpha_h \int_0^h \frac{dz}{[n^2(z) - \cos^2 \alpha_0]^{1/2}} \int_0^h \frac{n^2(z)\, dz}{[n^2(z) - \cos^2 \alpha_0]^{3/2}}}. \tag{8}$$

For angles of incidence $\beta = 90° - \alpha$ expression (8) has the form

$$\eta = \frac{r^2}{\cos \beta_0 \cos \beta_h \int_0^h \frac{dz}{[n^2(z) - \sin^2 \beta_0]^{1/2}} \int_0^h \frac{n^2(z)\, dz}{[n^2(z) - \sin^2 \beta_0]^{3/2}}}. \tag{8a}$$

Small Glancing Angles

In computing the focusing factor on the basis of expression (5) for small glancing angles we take into account that $R \approx r$.

$$\eta = \frac{R \cos \alpha_0}{\frac{\partial R}{\partial \alpha_0} \sin \alpha_h}. \tag{9}$$

Hence, using equations (6) and (7), we find

APPROVED FOR RELEASE: 2007/02/09: CIA-RDP82-00850R000500020040-0

APPROVED FOR RELEASE: 2007/02/09: CIA-RDP82-00850R000500020040-0

$$\eta = \frac{\cos^2 \alpha_0 \int_0^h \frac{dz}{[n^2(z) - \cos^2 \alpha_0]^{1/2}}}{\sin \alpha_h \sin \alpha_0 \int_0^h \frac{n^2(z)\, dz}{[n^2(z) - \cos^2 \alpha_0]^{3/2}}}. \quad (10)$$

In the case of one refracting boundary n(z) = 1 with $0 \leqslant z < h_0$ and n(z) = n with $h_0 < z \leqslant h_0 + h_1$. Then expression (10), taking into account the ratio

$$\alpha_h = \frac{1}{n}(n^2 - \cos^2 \alpha_0)^{1/2}$$

assumes the form

$$\eta = \frac{n\left(\frac{h_0}{\operatorname{tg} \alpha_0} + \frac{h_1}{\operatorname{tg} \alpha_1}\right)}{\frac{\operatorname{tg} \alpha_1 \cdot h_0}{\sin^2 \alpha_0} + \frac{\operatorname{tg} \alpha_0 \cdot h_1}{\sin^2 \alpha_1}}, \quad (11)$$

where α_1 is the glancing angle with $h_0 < z \leqslant h_0 + h_1$.

Table 1

Focusing Factors and Attenuation of Signal During Its Propagation From Air Into Snow and Back (N)

Glancing angle, degrees	η_1	η_2	N, db
1	0.0232	0.0103	36.4
2	0.4640	0.0206	30.4
5	0.1160	0.0515	22.4
10	0.2300	0.1020	16.4

As an example, we will cite the results of computation of the focusing factor η_1 (in relative units) (Table 1) with passage of the radiation from a medium with the refractive index $n_{air} = 1$ (air) into a medium with a refractive index $n_{snow} = 1.5$ (snow with a density of about 0.5 g/cm^3) and back η_2 for $h_0 \geqslant h_1$ and different glancing angles in the first medium (air). The relative refractive indices will be: with propagation from the air into the snow $n = n_{snow}/n_{air} = 1.5$, with "backward" propagation $n' = n_{air}/n_{snow} = 0.67$.

In this case (with $h_0 \geqslant h_1$), assuming $\cos^2 \alpha_0 = 1$ and neglecting the terms containing t the second and third powers of sin α_0, expression (11) can be reduced to the extremely simple form

$$\eta = \eta_{11} = \frac{\sin \alpha_0}{\sin \alpha_1}. \quad (12)$$

For the propagation of waves from the snow into the air (the point of emergence is in the snow, the glancing angle is α'_0; the observation point is in the air, the glancing angle is α'_1) we have

APPROVED FOR RELEASE: 2007/02/09: CIA-RDP82-00850R000500020040-0

APPROVED FOR RELEASE: 2007/02/09: CIA-RDP82-00850R000500020040-0

$$\eta_2 = n'^2 \frac{\sin \gamma_1'}{\sin \gamma_0'}$$

or, returning to the annotations adopted earlier, corresponding to a point of emergence situated in the air,

$$\eta_2 = \frac{1}{n^2} \cdot \frac{\sin \gamma_0}{\sin \gamma_1}. \tag{13}$$

Then the attenuation of the signal N (db) in the case of its propagation in "forward" and "backward" directions is

$$N = 10 \lg \eta_1 \eta_2 = 10 \lg \frac{\sin \gamma_0}{n^2 \sin \gamma_1}.$$

Small Angles of Incidence (Vertical Sounding)

In those cases when n(z) is a step function, it is convenient to use the following form of expression (8a)

$$\eta = \frac{r^2 \sin \beta_0}{\cos \beta_h \int_0^h \operatorname{tg} \beta_h \, dz \int_0^h \frac{\cos \beta_0 \, dz}{n(z) \cos^2 \beta_h}}. \tag{14}$$

For the case of a plane boundary between two homogeneous media (n(z) = 1 with $0 \leqslant z < h_0$ and n(z) = n with $h_0 < z \leqslant h_0 + h_1$) expression (14) has the form

$$\eta = \frac{r^2 \sin \beta_0}{\cos \beta_1 (h_0 \operatorname{tg} \beta_0 + h_1 \operatorname{tg} \beta_1) \left(\frac{h_0 \cos \beta_0}{\cos^3 \beta_0} + \frac{h_1 \cos \beta_0}{n_1 \cos^3 \beta_1} \right)}. \tag{15}$$

We will determine the dependence of the focusing factor on the ratio of h_0 and h_1 and the coefficient of refraction n. With small angles of incidence the following expressions are correct:

$$r = h_0 + h_1;$$

$$\left.\begin{aligned} \operatorname{tg} \beta_0 &\approx \sin \beta_0 \approx \beta_0 \\ \operatorname{tg} \beta_1 &\approx \sin \beta_1 \approx \beta_1 \end{aligned}\right\} \frac{\beta_0}{\beta_1} = n;$$

$$\cos \beta_0 \approx \cos \beta_1 \approx 1.$$

With these equations taken into account, from expression (15) we obtain the focusing factor

$$\eta = \frac{\left(1 + \frac{h_1}{h_0}\right)^2}{\left(1 + \frac{1}{n} \cdot \frac{h_1}{h_0}\right)^2}. \tag{16}$$

We will find the focusing factor for the case of vertical radio echo sounding of the medium from the air. With propagation of the wave from the antenna to the reflecting object in the medium the focusing factor accordingly is equal to

APPROVED FOR RELEASE: 2007/02/09: CIA-RDP82-00850R000500020040-0

APPROVED FOR RELEASE: 2007/02/09: CIA-RDP82-00850R000500020040-0

$$\eta_{\max} = \frac{\left(1 + \frac{h_c}{h_a}\right)^2}{\left(1 + \frac{1}{n} \cdot \frac{h_c}{h_a}\right)^2}, \tag{17}$$

[a = antenna; c = layer]

where $h_a = h_0$ is the height of the antenna above the air-medium boundary; $h_{1ay} = h_1$ is the thickness of the sounded layer of the medium; n is the relative coefficient of refraction of the sounded medium.

With propagation of the wave from the reflecting object in the medium to the antenna the "backward" focusing factor is

[OTP = refl; a = antenna; c = layer]

$$\eta_{\text{отр}} = \frac{\left(1 + \frac{h_c}{h_a}\right)^2}{n^2\left(1 + \frac{1}{n} \cdot \frac{h_c}{h_a}\right)^2}. \tag{18}$$

The focusing factor in sounding of the medium is equal to the product of the focusing factors during the propagation of the wave in "forward" and "backward" directions

[пад = incid; OTP = refl]

$$\eta' = \eta_{\max}\eta_{\text{отр}} = \frac{\left(1 + \frac{h_c}{h_a}\right)^4}{n^2\left(1 + \frac{1}{n} \cdot \frac{h_c}{h_a}\right)^4}. \tag{19}$$

It should be noted that the expressions for the focusing factor (17), (18) and (19) were obtained for a point isotropic sound source situated at the point where the antenna is located (focusing of direct signal), or at the point where the reflecting object is situated (focusing of the reflected signal), and do not take into account the changes in the effective reflecting surface of the object, which can occur with a replacement of the real inhomogeneous medium by a homogeneous medium.

Change in Effective Reflecting Area of Some Objects in an Inhomogeneous Medium

Case of mirror reflecting plane. The effective reflecting area (S_{eff}) of the mirror plane is determined by the expression $S_{eff} = \pi r^2$. [In general $S_{eff} = \pi r^2 K_f^2$, where K_f is the Fresnel coefficient. The Fresnel losses can be taken into account separately and are not considered here.] In a homogeneous medium r is the distance from the source to the plane, in an inhomogeneous medium r is the radius of curvature of the wave front or the distance to a fictitious source; in the case of vertical propagation of a wave in the air and a homogeneous medium with the refractive index n $r \approx h_a n + h_{layer}$.

The change in the effective reflecting area in an inhomogeneous medium will be characterized by the ratio $\xi = S_{eff\ med}/S_{eff}$, where S_{eff} is the effective reflecting area of the object in the air; $S_{eff\ med}$ is the effective reflecting area in a particular inhomogeneous medium with a constant spatial positioning of the object relative to the sounder antenna.

The parameter ξ for a mirror reflecting plane, in accordance with what has been said above, is equal to

[c = layer; a = antenna]

$$\xi = \frac{n^2\left(1 + \frac{1}{n} \cdot \frac{h_c}{h_a}\right)^2}{\left(1 + \frac{h_c}{h_a}\right)^2}. \tag{20}$$

APPROVED FOR RELEASE: 2007/02/09: CIA-RDP82-00850R000500020040-0

APPROVED FOR RELEASE: 2007/02/09: CIA-RDP82-00850R000500020040-0

The focusing factor from expression (19), taking into account the change in the effective reflecting plane (20), in the case of vertical sounding of the medium with a plane mirror lower boundary, is equal to

$$\eta' = \eta_{\text{пад}}\eta_{\text{отр}}\xi = \frac{\left(1+\frac{h_c}{h_a}\right)^2}{\left(1+\frac{1}{n}\cdot\frac{h_c}{h_a}\right)^2}. \qquad (21)$$

[пад= inc(ident); отр = refl]

Case of scattering plane surface. When the scattering plane surface is situated in the near zone of the sounder its effective reflecting area is determined as $S_{eff} = \pi r^2$. In this case for the focusing factor expression (21) is correct.

However, when the scattering plane is situated in the far zone of the sounder, the effective reflecting area is determined using the formula

$$S_{eff} = \sigma_0 \pi r c \tau_{pulse}/2n, \qquad (22)$$

where σ_0 is the specific effective area; c is the velocity of electromagnetic waves in the air; τ_{pulse} is sounder pulse duration.

For the case of sounding of the medium from the air $r \approx nh_a + h_{layer}$, $n = n_{layer}$ and accordingly, the ξ parameter for the scattering plane in the far zone of the sounder is

$$\xi = \frac{\left(1+\frac{1}{n}\cdot\frac{h_c}{h_a}\right)}{\left(1+\frac{h_c}{h_a}\right)}. \qquad (23)$$

[c = layer; a = antenna]

Using expressions (19) and (23) we find that the focusing factor, taking into account the change in the effective reflecting surface during sounding of a medium with a scattering plane lower boundary situated in the far zone of the sounder, is

$$\eta' = \frac{\left(1+\frac{h_c}{h_a}\right)^3}{n^2\left(1+\frac{1}{n}\cdot\frac{h_c}{h_a}\right)^3}. \qquad (24)$$

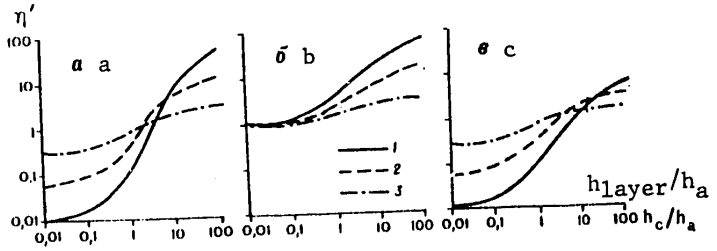

Fig. 1. Focusing factor η' in case of vertical radio echo sounding of media with different refractive indices n (1 -- n = 9; 2 -- n = 4; 3 -- n = 1.79). a) isotropic reflector; b) mirror reflection and scattering plane in near zone; 3) scattering plane in far zone.

Figure 1 shows the dependence of the focusing factor η' on the ratio of the thickness of the layer of the medium to the height of rising of the antenna above the upper boundary of the sounded medium in accordance with the expressions (19), (21) and (24). Analyzing these dependences, it can be concluded that with vertical

APPROVED FOR RELEASE: 2007/02/09: CIA-RDP82-00850R000500020040-0

APPROVED FOR RELEASE: 2007/02/09: CIA-RDP82-00850R000500020040-0

sounding of the medium from the air the contribution of the focusing factor to the total attenuation of the radio echo signal in all cases is from -20 lg n to +20 lg n. For ice it is equal to from -6 to +6 db; therefore, the circumstance that some authors (for example, the author of [1]) did not take the focusing factor into account (although it was mentioned) in computations of the total attenuation of the radio echo signal in a glacier, did not lead to such great errors as would cause a serious discrepancy between the computed and experimental data. However, without question, the dependence of the focusing factor on the ratio h_{layer}/h_a is one of the reasons for the appreciable change in attenuation of the radio echo signal observed in practical work with an increase in aircraft flight altitude during radio echo measurements of the thickness of glaciers. In part, therefore, a survey of thicknesses is usually made from aircraft flying low over the surface of glaciers.

It follows from expressions (19), (21) and (24) that it is always relatively more advantageous (bearing in mind only the focusing factor) to sound thick layers than to sound thin layers. This must be taken into account when sounding floating sea and fresh ice. The influence of the focusing factor should be extremely important in the sounding of media with large n values, for example, for fresh water, for which at frequencies in the meter wavelength region $n \approx 9$.

BIBLIOGRAPHY

1. Bogorodskiy, V. V., FIZICHESKIYE METODY ISSLEDOVANIYA LEDNIKOV (Physical Methods for Investigating Glaciers), 1967, 214 pages.

2. Brekhovskikh, L. M., VOLNY V SLOISTYKH SREDAKH (Waves in Layered Media), Moscow, Izd-vo AN SSSR, 1957, 503 pages.

3. Finkel'shteyn, M. I. and Kutev, V. A., "Sounding of Sea Ice Using a Series of Videopulses," RADIOTEKHNIKA I ELEKTRONIKA (Radio Engineering and Electronics), Vol XVII, No 10, pp 2107-2112, 1972.

4. Evans, S., "Progress Report on Radio Echo Sounding," POLAR RECORD, Vol 13, No 85, pp 413-420, 1967.

COPYRIGHT: Arkticheskiy i antarkticheskiy nauchno-issledovatel'skiy institut (AANII), 1975

APPROVED FOR RELEASE: 2007/02/09: CIA-RDP82-00850R000500020040-0

APPROVED FOR RELEASE: 2007/02/09: CIA-RDP82-00850R000500020040-0

TOTAL SIGNAL ATTENUATION IN RADIO ECHO SOUNDING OF GLACIERS

Leningrad TRUDY. ORDENA LENINA ARKTICHESKIY I ANTARKTICHESKIY NAUCHNO-ISSLEDOVATEL'-SKIY INSTITUT. RADIOFIZICHESKIYE METODY ISSLEDOVANIY VODNYKH MASS SNEGA I L'DA in Russian No 324, 1974 pp 12-19

[Article by V. V. Bogorodskiy, G. V. Trepov and B. A. Fedorov]

[Text] The problem of the total attenuation of a signal is extremely important in refining a model of radio wave propagation during radio echo sounding of media, investigation of the electric characteristics of ice, and also in selecting frequencies and potentials of sounding apparatus for the sounding of glaciers. On the basis of the general concepts of the theory of radio wave propagation and considerable material on the attenuation of electromagnetic waves during the radio echo sounding of glaciers it is possible to visualize the following additive mechanisms of signal attenuation.

1. Geometrical losses due to spatial divergence of the wave front (N_{geo}).
2. Losses due to focusing, caused by refraction at the air-glacier surface boundary and a change of density in the upper part of the glacier (N_{foc}).
3. Absorption (N_{abs}).
4. Losses with reflection from the glacier-glacier bed boundary (N_{refl}).
5. Scattering by the glacier surface and inhomogeneities within it (N_{scat}).
6. Noncoincidence of the polarization of the reflected signal and polarization of the receiving antenna as a result of wave depolarization during propagation in the glacier (N_{pol}).

For geometrical losses and losses accompanying reflection in the case of mirror reflection and scattering when working in the near zone

$$(h < [20\text{-}30]\ \frac{c\tau_{pulse}}{2})$$

in accordance with $S_{eff} = \pi h^2 k_f^2$ we have

$$N_{geo} + N_{refl} = 20 \lg G\lambda + 20 \lg h + 10 \lg 64\pi^2 - 20 \lg k_f, \quad (1)$$

where c is the speed of light in a vacuum; τ_{pulse} is sounder pulse duration; S_{eff} is the effective reflecting area; h is glacier thickness; k_f is the Fresnel coefficient of the ice-bed boundary; G is the antenna amplification factor; λ is the working wavelength of the sounder.

APPROVED FOR RELEASE: 2007/02/09: CIA-RDP82-00850R000500020040-0

APPROVED FOR RELEASE: 2007/02/09: CIA-RDP82-00850R000500020040-0

The losses $N_{refl} = -20 \lg k_f$ are dependent on the dielectric constant of the underlying surface. With a change in the relative dielectric constant of rocks ε'_{rock} from 6 to 9 N_{refl} changes from 16.2 to 11.8 db; here for the computations it was assumed that $N_{refl} = 14$ db. Summing the components of geometrical losses and losses during reflection, we obtain

$$N_{geo} + N_{refl} = -20 \lg G\lambda + 20 \lg h + 42 \text{ (db)}. \quad (2)$$

The losses due to focusing are $N_{foc} = -10 \lg \eta$ [1] at the surface of the glacier and constitute 5 db. When working from an aircraft it is necessary to take into account their change with altitude.

Absorption is determined by the thickness and temperature regime of the glacier. If the temperature distribution in the thickness of the glacier is known, absorption can be computed using the expression

$$N_{abs} = \int_0^h \overline{N}_{abs} |t(z)| dz. \quad (3)$$

Usually the temperature distribution is unknown and therefore the absorbing properties of the thickness of the glacier will correspond to the absorption temperature t_{abs} satisfying the expression

$$N_{abs} = \overline{N}_{abs}(t_{abs})h.$$

The $\overline{N}_{abs}(t_{abs})$ values were computed on the basis of the equation

$$\overline{N}_{abs} = 8{,}68 \frac{2\pi}{c} f \operatorname{tg}\delta \sqrt{\varepsilon'} \quad \text{(db/m)},$$

where $\operatorname{tg}\delta$ is the tangent of the angle of dielectric losses; ε' relates to the glacier as a whole.

The specific absorption $\overline{N}_{abs}$ for glacier ice in the range of meter and decimeter waves (from 10 to 500 MHz) is given below:

t_{abs}, °C	-1	-5	-10	-20	-30	-40	-50	-60
$\overline{N}_{abs}(t_{abs})$, db/m	0.1062	0.0709	0.050	0.0322	0.0209	0.0129	0.0077	0.0025

In the computations we used the results obtained by Westphal [3] and extrapolation was carried out using the Debye formulas.

Scattering by the glacier surface is characterized by the Fresnel coefficient for the air-ice boundary

$$N_{scat} = -20 \lg (1 - k_f^2) = 0{,}7 \text{ (db)} \quad (4)$$

where

[B = air] $$k_f = \frac{\sqrt{\varepsilon'} - \sqrt{\varepsilon'_n}}{\sqrt{\varepsilon'} + \sqrt{\varepsilon'_n}} = 0{,}283;$$

ε' and ε'_{air} -- the relative dielectric constants of ice and air respectively.

In some cases, for example during thawing, scattering at the upper boundary can be considerably greater.

APPROVED FOR RELEASE: 2007/02/09: CIA-RDP82-00850R000500020040-0

APPROVED FOR RELEASE: 2007/02/09: CIA-RDP82-00850R000500020040-0

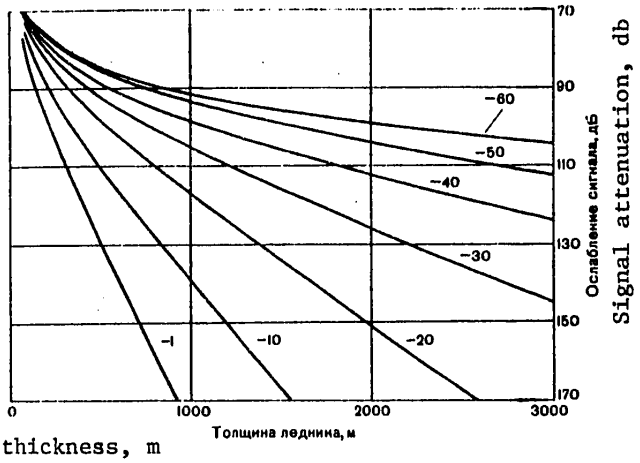

Fig. 1. Total attenuation of radio echo signal in glacier for different absorption temperatures (t_{abs} from -1 to -60°C) for case of sounding from surface transport.

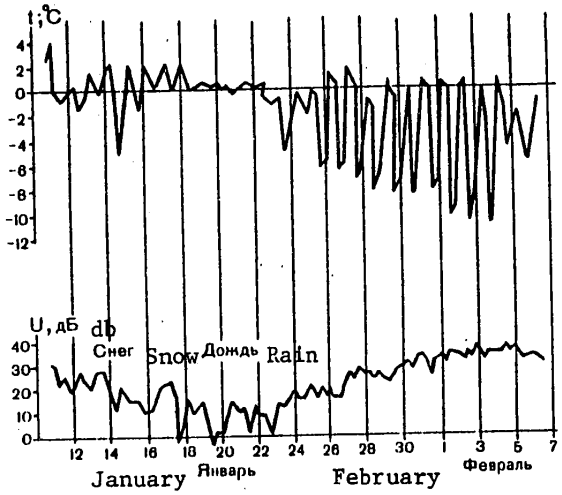

Fig. 2. Air temperature near glacier surface t and level of the reflected signal U.

With the reception of waves with an arbitrary polarization with a linear dipole the losses N_{pol} on the average are 3 db (with a uniform distribution of angles between the polarization plane of the receiving dipole and the received signal).

Thus, the total attenuation, as a function of the sounder parameters, thickness of the glacier and temperature, can be written in the form

APPROVED FOR RELEASE: 2007/02/09: CIA-RDP82-00850R000500020040-0

APPROVED FOR RELEASE: 2007/02/09: CIA-RDP82-00850R000500020040-0

$$N_{\Sigma} = N_{geo} + N_{refl} + N_{abs} + N_{foc} + N_{pol} + N_{scat} = -20 \lg G\lambda + \quad (5)$$

$$+20 \lg h + N_{abs}(t_{abs})h+40.7 \text{ (db)}.$$

The results of computations of N_{Σ} in accordance with expression (5) are represented in Fig. 1. For the computations it was assumed that $G\lambda = 10$.

The total attenuation, in general, is a random value and this is manifested in fluctuations of the reflected signal, but the great number of measurements of the total attenuation makes it possible to carry out averaging and check the correctness of the adopted computation model under different conditions (thickness of glacier, mean annual temperature, parameters of apparatus). In addition, the contribution of some mechanisms can be determined from special experiments.

An investigation of the influence of temperature of the surface layer of the glacier on attenuation of the radio signal was carried out in the neighborhood of Mirnyy Observatory in Antarctica from 11 January through 6 February 1967 at a frequency of 440 MHz. The collected data on the excess of the signal over the receiver noise and air temperature near the ice surface are given in Fig. 2. The results of the experiment show that at a frequency of 440 MHz there is a strong dependence of attenuation of the radio echo signal on the temperature of the surface layer of the glacier. With thawing at the glacier surface the attenuation increases. The greatest increments in attenuation (about 20 db) were registered with the falling of precipitation in the form of rain or snow mixed with rain. The maximum attenuation of the radio echo signal in the surface layer of a thawing glacier is more than 30 db. Similar results were obtained during the Eleventh Soviet Antarctic Expedition, when after the falling of rain the maximum thicknesses attainable when making measurements at a frequency of 440 MHz decreased from 300-350 m to 100-150 m (near the shore), which corresponds to an increase in attenuation by 20 db or more.

For an investigation of attenuation of the radar signal in a broad frequency range on the Fourteenth Soviet Antarctic Expedition on a path with an extent of 132 km to the south of Molodezhnaya Station specialists carried out sounding of the glacier by means of a multifrequency sounder and a sounder with a working frequency of 60 MHz. [Some results were published in [2].] From a comparison of the total attenuation of the radio echo signal with sounding at six frequencies it is possible to draw the following conclusions.

1. The curves of change in attenuation along the path for frequencies of 60, 70, 100, 140, 200, 440 MHz are similar and are very strongly correlated with glacier thickness.

2. On the average the difference in signal levels in db at different frequencies is almost constant, regardless of the glacier thickness (220-950 m) and its mean annual temperature (t_{mean} from -4 to -25°C), that is, the temperature dependence of total attenuation and its dependence on thickness are approximately identical at frequencies from 60 to 440 MHz.

3. The strong dependence of total attenuation on temperature is confirmed; for example, whereas at the 10th kilometer (t_{mean} = -8°C) a signal level of 10 db corresponded to a thickness of 240 m, at the 24th kilometer (t_{mean} = 16°C) it

APPROVED FOR RELEASE: 2007/02/09: CIA-RDP82-00850R000500020040-0

APPROVED FOR RELEASE: 2007/02/09: CIA-RDP82-00850R000500020040-0

corresponds to 440 m, at 60 m (t_{mean} = -19°C) -- 850 m, at 128 m (t_{mean} = -25°C) -- 900 m.

4. In the coastal zone (approximately to kilometer 15) the difference in total attenuations for low and high frequencies increases. The losses at low frequencies (100, 70 MHz) become smaller relative to those for the higher frequencies.

A comparison of the computed values of total attenuation obtained on the basis of expression (5) for absorption temperatures t_{abs} equal to $0.75t_{mean}$ and $0.9t_{mean}$ and experimental data shows that:
-- the general shape of the computed and experimental curves is identical;
-- in the sector to the 15th kilometer the experimentally determined attenuation is greater than the computed value for $t_{abs} = 0.75t_{mean}$ by 3-12 db, which can be attributed to scattering in the upper thawing layer of the glacier; losses in the upper layer increase with an increase in frequency and with approach to the shoreline;
-- in the sector 15-48 km, 59-69 km, 114-116 km the data computed for $t_{abs} = 0.75t_{mean}$ and the experimental data coincide on the average with an accuracy to 2-4 db;
-- in the sector 121-130 km the measured attenuation is less than the computed value for $t_{abs} = 0.75t_{mean}$ by 3-6 db; in this sector the absorption temperature for the glacier falls in the range $0.75t_{mean} < t_{abs} < 0.9t_{mean}$.

The results of experimental measurements of the total attenuation of a radio echo signal at frequencies 60, 70, 100, 140, 200 and 440 MHz and comparison of the computed data with the experimental data indicate the correctness of the adopted model of signal propagation during the sounding of glaciers. In accordance with this model it follows that:

1. The geometrical losses were computed using the law $1/h^2$.
2. It is necessary to take into account the focusing factor, as demonstrated in [1] (for sounding of the glacier directly from its surface the gain due to focusing is 5 db).
3. The losses with reflection from the glacier bed must be taken into account in accordance with expression (1).
4. The losses in scattering must be considered approximately 1 db for cold glaciers and must be considered to increase to 20-30 db when there is thawing at the surface.
5. When computing absorption it is necessary to know the absorption temperature; it can vary in some limits, such as 0.75-0.9 of the mean annual value, which does not cause significant errors in computing total attenuation.

However, it is more correct to solve the inverse problem: using all the remaining components of total attenuation, discriminate from the measured attenuation the losses in absorption and ascertain the absorption temperature, which characterizes the temperature regime of the glacier.

During subsequent Antarctic Expeditions (Fifteenth, Sixteenth and Seventeenth) the measurements of attenuation were made along the same route as on the Fourteenth Expedition, at frequencies of 60, 213 and 440 MHz. In the generalization we used random samples of attenuations. Qualitatively (and quantitatively with an accuracy to the range of fluctuations of amplitude) these results coincided with those

APPROVED FOR RELEASE: 2007/02/09: CIA-RDP82-00850R000500020040-0

APPROVED FOR RELEASE: 2007/02/09: CIA-RDP82-00850R000500020040-0

cited above. Particular attention should be given to data on attenuation determined by A. M. Shalgin and L. A. Fedorinchik in the neighborhood of Mirnyy station in 1971/1972 in polygons measuring 5 x 5 km, situated at the 57th and 153d km from the shoreline. Measurements in each polygon were made along 22 intersecting lines at intervals of 250 m. Samples were taken from the observational series for the ranges in glacier thickness Δh = 100 m. In selecting the Δh interval it was taken into account that, on the one hand, the samples should be adequately long, but on the other hand, the Δh value cannot be too great since in this case the regular change in signal amplitude caused by the dispersion of electromagnetic energy will be great.

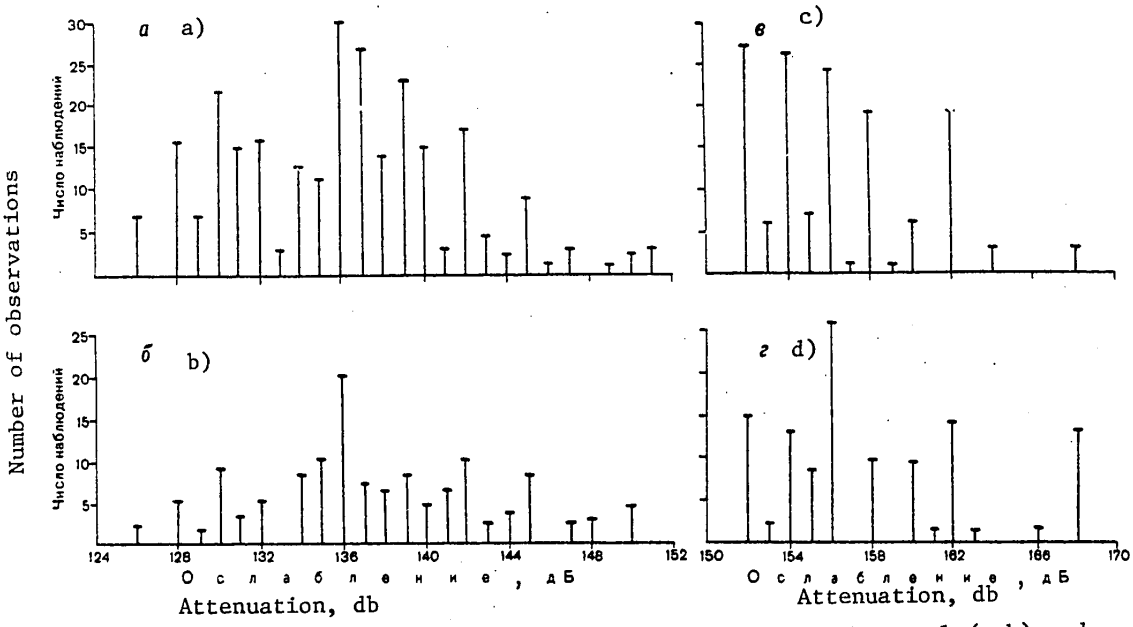

Fig. 3. Histograms of attenuations of radio echo signals in polygons 1 (a,b) and 2 (c,d). a) Δh = 950-1050 m; b) Δh = 1050-1150 m; c) Δh = 1750-1850 m; d) Δh = 1850-1950 m.

Figure 3 shows the distribution of probabilities (repetition rates) of attenuation of radio echo signals for polygons 1 and 2. It is characterized by a variability of attenuation caused by the influence of random factors (scattering, depolarization) in the case of a constant temperature regime of the glacier (t_{abs} = const) and an approximately constant thickness ($h \approx$ const). Figure 3 shows that the probabilities of attenuation have a Rayleigh distribution. In polygon 1 the mean attenuation values are 136 and 138 db for mean thicknesses of 1000 and 1100 m, in polygon 2 -- about 157 db for thicknesses of 1800 and 1900 m. These mean attenuation values once again confirm the correctness of the adopted attenuation computation scheme; they correspond to glacier absorption temperatures t_{abs} = -11°C for polygon 1 and t_{abs} = -16°C for polygon 2, not contradicting existing concepts concerning the thermal regime of the glacier in the measurement regions.

APPROVED FOR RELEASE: 2007/02/09: CIA-RDP82-00850R000500020040-0

APPROVED FOR RELEASE: 2007/02/09: CIA-RDP82-00850R000500020040-0

BIBLIOGRAPHY

1. Bogorodskiy, V. V., Trepov, G. V. and Fedorov, B. A., "Focusing Factor in Radio Echo Sounding of Media," in this collection of articles.

2. Bogorodskiy, V. V., Trepov, G. V. and Fedorov, B. A., "On Measuring Dielectric Properties of Glaciers in the Field," PROC. OF THE INTERNATIONAL MEETING ON RADIOGLACIOLOGY LYNGBY, pp 20-31, 1970.

3. Ragle, R. H., et al., "Ice Core Studies of Ward Hunt Island Ice Shelf," 1960. [By R. H. Ragle, R. G. Blair and L. E. Persson], JOURNAL OF GLACIOLOGY, Vol 5, No 37, pp 39-59, 1964.

COPYRIGHT: Arkticheskiy i antarkticheskiy nauchno-issledovatel'skiy institut (AANII), 1975

APPROVED FOR RELEASE: 2007/02/09: CIA-RDP82-00850R000500020040-0

APPROVED FOR RELEASE: 2007/02/09: CIA-RDP82-00850R000500020040-0

FLUCTUATIONS OF AMPLITUDE OF REFLECTED RADIO ECHO SIGNALS IN SOUNDING OF GLACIERS

Leningrad TRUDY. ORDENA LENINA ARKTICHESKIY I ANTARKTICHESKIY NAUCHNO-ISSLEDOVATEL'-SKIY INSTITUT. RADIOFIZICHESKIYE METODY ISSLEDOVANIY VODNYKH MASS SNEGA I L'DA in Russian No 324, 1974, pp 20-27

[Article by V. V. Bogorodskiy, G. V. Trepov and B. A. Fedorov]

[Text] Radio echo sounding of glaciers is carried out in the meter wavelength range [1]. When the resolution of the sounder is small in range and angle the structure of the signal received from the glacier bed region is quite complex. The echo signal is a series of resolved pulses with an amplitude which in general decreases. [By "resolved" is meant pulses whose peaks are resolved on the oscillogram.] If the sounder is moved horizontally, the echo signal fluctuates and its different parts fluctuate differently [5, 6]. This phenomenon has been called "spatial fading" [6]. The reasons for this are unevenness of the bed, the presence of morainal inclusions, and also a change in signal polarization [2], nonuniformity of the glacier, etc.

A study by Walford [6] discusses an interesting practical application of "spatial fading." In particular, it was shown (and this has been confirmed by data from geodetic measurements) that with the carrying out of repeated registration of a bottom signal along paths it is possible to determine the displacement of the glacier surface relative to the bedrock relief.

With respect to fluctuations per se, Walford determined the periodic length L of fadings of signals as functions of the partial time τ from the moment of arrival of an echo (for a point with a glacier thickness of about 1090 m). For a theoretical estimate of the L value Walford used an expression from an unpublished study by Berry:

$$L = \frac{\lambda}{2\sqrt{2}} \cdot \frac{h + \frac{1}{2} v\bar{\tau}}{\sqrt{\frac{1}{2} v\tau \left(2h + \frac{1}{2} v\tau\right)}}, \qquad (1)$$

where v is the velocity of propagation of a radio echo signal in the ice; λ is the length (in the ice) of the sounder working wave; h is glacier thickness; τ is partial time; $\bar{\tau}$ was determined by Berry, and in Walford's words, "differs negligibly from τ" when computing L.

There can be a different approach to the problem of study of fluctuations of bottom signals, and, in particular, fluctuations of their amplitude. It appears that a knowledge of the characteristics of spatial fading, such as the statistical

APPROVED FOR RELEASE: 2007/02/09: CIA-RDP82-00850R000500020040-0

APPROVED FOR RELEASE: 2007/02/09: CIA-RDP82-00850R000500020040-0

characteristics, can exert a substantial influence on solution of a number of problems of practical importance, such as the choice of frequencies for measurements of displacement of the surface, evaluation of the effectiveness of accumulation of the energy of reflected signals during the sounding of a glacier from surface transportation and an aircraft and estimation of the size of irregularities of the bed comparable with the wavelength of the irradiating wave.

Such an approach also determined the conditions for conducting the experiment.

Table 1

Experimental Values of Period (L) of Spatial Fading of Arrival Pulse of Bottom Echo Signal

Glacier thickness, m	Frequency 60 MHz: $\lambda = 2.8$ m, $\tau_{pulse} = 1\mu$sec		Frequency 213 MHz: $\lambda = 0.79$ m, $\tau_{pulse} = 2.5\mu$sec		Frequency 440 MHz: $\lambda = 0.38$ m, $\tau_{pulse} = 0.3\mu$sec	
	L	L_{mean}	L	L_{mean}	L	L_{mean}
300	2.8; 2.3	2.55	1.2; 1.3	1.25	1.0; 0.8 0.5; 1.4	0.92
600	7.0; 3.4 3.0; 1.6	3.75	1.9	1.9	1.6; 1.2 1.3; 1.0	1.28
850	2.4; 2.0 3.0; 3.0 2.2; 2.2	2.55	2.0	2.0	0.7	0.7
1225	5.0; 5.2 6.5; 4.0	5.17	2.0; 2.8	2.4	--	--
1250	3.6; 6.2 4.4; 4.2	4.6	2.4; 1.6	2.0	--	--
1900	3.6; 9.6 5.6; 6.0	6.2	2.0	2.0	--	--

Note: Each L value with one and the same thickness is given for different measurement paths.

First, for carrying out a frequency analysis of signal fluctuations we used multifrequency sounding: frequencies 60, 213 and 440 MHz.

Second, for the purpose of clarifying the stability of spatial fading and the dependence of the statistical characteristics, especially the autocorrelation radius of amplitude fluctuations, on glacier thickness the sounding was carried out at several points where the ice thicknesses were different.

Third, since the electromagnetic signal, in propagating in the glacier, changes its polarization and the nature of the relief is hypothetically different in the directions of the flow lines of the glacier and perpendicular to it, two lines were run at each measurement point: north-south and east-west.

APPROVED FOR RELEASE: 2007/02/09: CIA-RDP82-00850R000500020040-0

APPROVED FOR RELEASE: 2007/02/09: CIA-RDP82-00850R000500020040-0

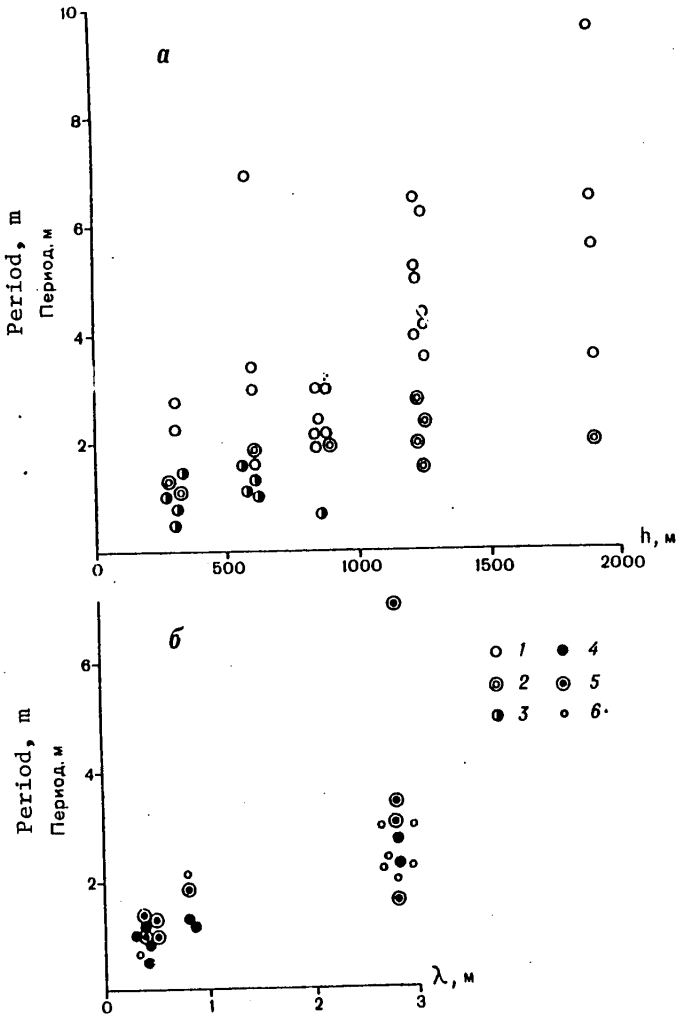

Frequency: 60 MHz (1); 213 MHz (2); 440 MHz (3). Thickness of glacier: 300 m (4); 600 m (5); 850 m (b).

Fig. 1. Experimental dependences of periods of spatial fading of arrival pulses of bottom echo signal on glacier thickness (a) and wavelength (b).

The measurements were made on the Sixteenth Soviet Antarctic Expedition in 1971 [4]. The work region was Molodezhnaya Station-Kilometer 105 to the south of Molodezhnaya. Signals from the oscillograph screen were registered on photographic film with movement of the transport vehicle with the sounders along paths whose length in different experiments was from 20 to 100 m. The registry frequency was 200-250 frames per 100 m of path; an amplitude signal mark was used; scanning was type A.

In processing of the collected data attention was concentrated on the first pulse -- the echo arrival pulse, since it, passing through the glacier along the shortest distance, carries the basic information and as a rule has the maximum

APPROVED FOR RELEASE: 2007/02/09: CIA-RDP82-00850R000500020040-0

APPROVED FOR RELEASE: 2007/02/09: CIA-RDP82-00850R000500020040-0

amplitude of all the resolved bottom pulses. For the first pulses we constructed "amplitude-distance" diagrams, histograms of amplitudes and autocorrelation functions. Among the autocorrelation characteristics we obtained the L values as the distances from the maximum of the autocorrelation function to the first minimum.

Table 1 gives the L values for frequencies 60, 213 and 440 MHz, as well as their mean arithmetical values L_{mean} for discrete ice thicknesses. Here we also give the lengths of the working waves of the sounder in the ice λ and the durations of the pulses τ_{pulse} radiated by them. Figure 1 show the experimental L values as functions of h and λ. The figure shows that the experimental L values do not fit into a linear dependence on λ, although it follows from expression (1) that there is a proportionality of L to the values λ, $\bar{h}$ and $1/\sqrt{\tau}$. In addition, it is unclear from expression (1) what value τ should have for the first resolved bottom signal. Clearly it is necessary to seek a suitable approximation of the experimental data represented in Fig. 1 and discuss its physical sense.

In order to obtain the initial expressions we will assume that in the case of an uneven bed, "bright" points (for example B and C in Fig. 2) participate in shaping of the echo signal; these points are situated in the glacier bed. During sounding $\Delta h = 1/2\ v\tau$, where τ is reckoned from the moment of echo arrival.

It follows from Fig. 2 that

$$\left.\begin{aligned} r &= h + \Delta h = h + \frac{1}{2} v\tau, \\ a &= \sqrt{2h\Delta h + (\Delta h)^2} = \sqrt{\frac{1}{2} v\tau \left(2h + \frac{1}{2} v\tau\right)}, \\ \frac{da}{d(\Delta h)} &= \frac{da}{dr} = \frac{h + \Delta h}{\sqrt{2h\Delta h + (\Delta h)^2}} = \frac{h + \frac{1}{2} v\tau}{\sqrt{\frac{1}{2} v\tau \left(2h + \frac{1}{2} v\tau\right)}}. \end{aligned}\right\} \quad (2)$$

Taking into account the signal propagation from the point A to the bed and back, we will determine the phase shift d (in wavelengths) for the increment dr: $d\varphi = 2/\lambda$ dr.

This phase shift corresponds to the spatial Doppler frequency

$$f_{max} = \frac{d\varphi}{da} = \frac{d\varphi}{dr} \cdot \frac{dr}{da} = \frac{2}{\lambda} \cdot \frac{\sqrt{\frac{1}{2} v\tau \left(2h + \frac{1}{2} v\tau\right)}}{h + \frac{1}{2} v\tau}. \quad (3)$$

For the "bright" points of the bed, situated at the angle α in plan to the direction of movement of the sounder (for example, the point D in Fig. 2),

$$f = f_{max} \cos\alpha,$$

hence

$$\alpha = \arccos \frac{f}{f_{max}}, \qquad \frac{df}{d\alpha} = f_{max}(-\sin\alpha),$$

and finally, taking into account that

APPROVED FOR RELEASE: 2007/02/09: CIA-RDP82-00850R000500020040-0

APPROVED FOR RELEASE: 2007/02/09: CIA-RDP82-00850R000500020040-0

$$\sin\arccos\frac{f}{f_{max}}=\sqrt{1-\left(\frac{f}{f_{max}}\right)^2},$$

$$d\alpha=\frac{df}{f_{max}(-\sin\tau)}=-\frac{\lambda}{2}\cdot\frac{h+\frac{1}{2}v\tau}{\sqrt{\frac{1}{2}v\tau\left(2h+\frac{1}{2}v\tau\right)}}\times$$

$$\times\frac{df}{\sqrt{1-\left(\frac{f}{f_{max}}\right)^2}}. \qquad (4)$$

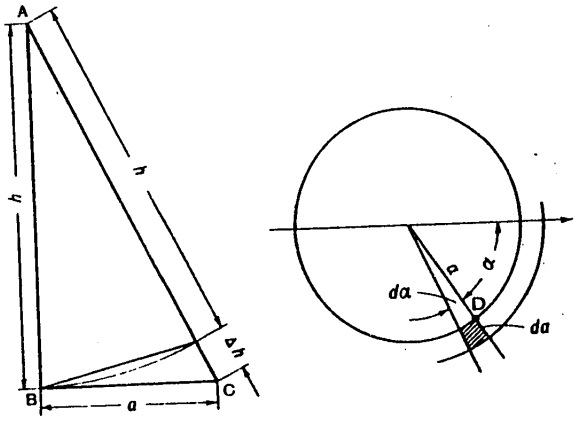

Fig. 2. Diagram explaining derivation of expression for period of spatial fading of arrival pulse of bottom echo signal.

The power reflected from an element of the ring adadα (this sector is shaded in Fig. 2), on the assumption of an invariability of the power flux density P_0 within the limits of the element, will be

$$P=P_0 a\,da\,d\alpha,$$

or, converting from da and dα to the intervals (τ, τ + dτ) and (f, df), taking into account that

$$P(f,\tau)=-P_0\frac{\lambda}{2}\cdot\frac{\left(h+\frac{1}{2}v\tau\right)^2}{\sqrt{\frac{1}{2}v\tau\left(2h+\frac{1}{2}v\tau\right)}}\times$$

$$\times\frac{\frac{1}{2}v\tau}{\sqrt{1-\left(\frac{f}{f_{max}}\right)^2}}df\,d\tau. \qquad (5)$$

APPROVED FOR RELEASE: 2007/02/09: CIA-RDP82-00850R000500020040-0

APPROVED FOR RELEASE: 2007/02/09: CIA-RDP82-00850R000500020040-0

It can be seen from equation (5) that in the spectrum of fluctuations of signal amplitude from a ring with a width corresponding to $d\tau$ with τ = const, the upper frequencies f_{max} and those close to it are emphasized. Accordingly, the period of spatial fading from the ring L_{ring} will be close to $1/2f_{max}$; the factor 2 takes into account the presence of fluctuations of the frequencies f_{max} and $-f_{max}$ in the spectrum. Thus,

$$L_{ring} \approx \frac{1}{2f_{max}} = \frac{\lambda}{4} \cdot \frac{h + \frac{1}{2} v\tau}{\sqrt{\frac{1}{2} v\tau \left(2h + \frac{1}{2} v\tau\right)}}. \quad (6)$$

We will make a qualitative analysis of the spectrum of fluctuations for the first resolved bottom signal. We note first that the frequency f_{max} increases proportionally to $\sqrt{\tau}$, whereas the relative contribution of the distant rings to the spectrum of echo signal fluctuations for a number of obvious reasons decreases.

The period of fluctuations of the first signal L_1 will be determined by the upper spectral component $2f_{max}$* for maximum τ in the limits of the first resolved signal

$$L_1 \approx \frac{1}{2f_{max}\big|_{\tau = \tau_{max}}} = \frac{\lambda}{4} \cdot \frac{h + \frac{1}{2} v\tau\Big|_{\tau = \tau_{max}}}{\sqrt{\frac{1}{2} v\tau \left(2h + \frac{1}{2} v\tau\right)}\Big|_{\tau = \tau_{max}}}. \quad (7)$$

If it is taken into account that for the first signal in most practical cases $h \gg 1/2\ v\tau$, then

$$L_1 \approx \frac{\lambda}{4} \cdot \frac{\sqrt{h}}{\sqrt{v} \cdot \sqrt{\tau}\big|_{\tau = \tau_{max}}}. \quad (8)$$

Expression (8) is written not only as corresponding to the conditions of the experiments, but also as a more graphic representation. In particular, from this expression it can be seen clearly that for the first signal it is necessary that τ be determined in such a way that the L_1 values, computed using formulas (7) and (8), coincide with the experimental estimate of L.

If the first signal is resolved, the upper frequency in the spectrum of fluctuations of the first signal should not exceed the frequency which corresponds to $\tau_{max} = \tau_{pulse}$. Accordingly, the period of the spatial fading for the first signal can be determined as $L_1 = 1/2f_{max}$ with $\tau_{max} = \tau_{pulse}$. However, such an approach to the theoretical estimate of L is not confirmed by experimental data, according to which L obviously is not dependent on τ_{pulse}, in any case for the durations cited in Table 1.

Also unproductive is the idea of the use of diagrams of backscattering, not dependent on λ and h. [So it appears, extremely frequently for different types of surfaces, especially sea surfaces [3].] With such an assumption L is not dependent on

* Such a determination agrees with that adopted in the processing of experimental data.

APPROVED FOR RELEASE: 2007/02/09: CIA-RDP82-00850R000500020040-0

APPROVED FOR RELEASE: 2007/02/09: CIA-RDP82-00850R000500020040-0

h, which also contradicts the experimental data.

Such an approximation of τ_{max} when

$$\frac{\tau_{max}}{\lambda/v} = n, \tag{9}$$

is successful; here n has the sense of the number of periods of the radio pulse pulse duty factor introducing a substantial energy contribution to the first signal.

The n value is random, not explicitly dependent on h, λ and τ_{pulse}. It should be noted that since expression (8), with equation (9) taken into account, reads as follows

$$L_1 \approx \frac{\sqrt{\lambda} \cdot \sqrt{h}}{4\sqrt{n}}, \tag{10}$$

an estimate of n on the basis of experimental data must be accomplished in accordance with the fact of a proportionality of the L value to the root of n.

Two estimates of n for 40 and 37 results of measurements (of 42) are given in Table 2.

In this table $\sigma(\sqrt{n})$ is the standard deviation of the $\sqrt{n}$ values from the mean arithmetical value $\sqrt{n}$. The n_{mean} value corresponds to the mean arithmetical value $\sqrt{n}$ and n_{min} and n_{max} give the interval in which n falls with a probability 0.68. The legitimacy of these estimates is based on the approximate symmetry of the distribution of specific $\sqrt{n}$ values, computed on the basis of expression (10) relative to the maximum; the maximum of the distribution is attained with $\sqrt{n} \approx 3.4$; $n \approx 11.5$.

Expression (10) characterizes scattering on the bed in the case of vertical sounding of glaciers and makes it possible to predict the value of the period of spatial fading of the arrival signal.

Table 2

Number of results taken into account (of 42)	Mean arithmetical value $\sqrt{n}$	$\sigma(\sqrt{n})$	n_{mean}	n_{min}	n_{max}
40	3.50	1.14	12.2	5.6	21.5
37	3.42	0.72	11.7	7.3	17.2

However, it must be remembered that the n_{mean} value for different types of surfaces underlying the glacier can differ somewhat from that obtained in this study. In particular, it is possible to expect lesser n_{mean} values when sounding glaciers having a smoothed lower boundary, such as shelf glaciers, and large values when the bed is strongly incised.

APPROVED FOR RELEASE: 2007/02/09: CIA-RDP82-00850R000500020040-0

APPROVED FOR RELEASE: 2007/02/09: CIA-RDP82-00850R000500020040-0

BIBLIOGRAPHY

1. Bogorodskiy, V. V., FIZICHESKIYE METODY ISSLEDOVANIYA LEDNIKOV (Physical Methods for Investigating Glaciers), Leningrad, Gidrometeoizdat, 1968, 214 pages.

2. Bogorodskiy, V. V., Trepov, G. V. and Fedorov, B. A., "Tensor Electromagnetic Properties of Glacier Ice," TRUDY AANII (Transactions of the Arctic and Antarctic Scientific Research Institute), Vol 295, pp 120-124, 1970.

3. Zubkovich, S. G., STATISTICHESKIYE KHARAKTERISTIKI RADIOSIGNALOV, OTRAZHENNYKH OT ZEMNOY POVERKHNOSTI (Statistical Characteristics of Radio Signals Reflected From the Earth's Surface), Moscow, "Sovetskoye Radio," 1968, 240 pages.

4. Kluga, A. M., Trepov, G. V., Fedorov, B. A. and Khokhlov, G. P., "Some Results of Radar Sounding of Glaciers in Antarctica in the Summer of 1970/71," TRUDY SOV. ANTARKT. EKSPED. (Transactions of the Soviet Antarctic Expedition), Vol 61, pp 151-163, 1973.

5. Fedorov, B. A., "Use of Active Radio Echo Sounding for Studying Antarctic Glaciers," INFORM. BYUL. SOV. ANTARKT. EKSPED. (Information Bulletin of the Soviet Antarctic Expedition), No 62, pp 19-24, 1967.

6. Walford, M. E. R., "Glacier Movement Measured With a Radio Echo Technique," NATURE, Vol 239, No 5367, pp 93-95, 1972.

COPYRIGHT: Arkticheskiy i antarkticheskiy nauchno-issledovatel'skiy institut (AANII), 1975

APPROVED FOR RELEASE: 2007/02/09: CIA-RDP82-00850R000500020040-0

APPROVED FOR RELEASE: 2007/02/09: CIA-RDP82-00850R000500020040-0

INTERPRETATION OF EXPERIMENTAL DATA WHEN MEASURING INHOMOGENEOUS SEA ICE SAMPLES IN CENTIMETER RANGE

Leningrad TRUDY. ORDENA LENINA ARKTICHESKIY I ANTARKTICHESKIY NAUCHNO-ISSLEDOVATEL'SKIY INSTITUT. RADIOFIZICHESKIYE METODY ISSLEDOVANIY VODNYKH MASS SNEGA I L'DA in Russian No 324, pp 28-32

[Article by V. V. Bogorodskiy and G. P. Khokhlov]

[Text] In an investigation of the electrical parameters of saline ice in free space by means of apparatus operating in the centimeter range it has been noted that the degree of homogeneity of the properties of ice in the thickness of samples exerts a great influence on the character of the primary experimental data.*

In the measurement of homogeneous samples with sufficiently great absorption the dependences of the displacement X of the minimum of the standing wave in the measurement line and attenuation T on sample thickness d have the form of straight lines. Using these dependences it is easy to determine the relative dielectric constant ε' and the tangent of the angle of losses tg δ:

[B = waveguide]

$$\varepsilon' = \left(1 + \frac{2\Delta X}{\Delta d} \cdot \frac{\lambda}{\lambda_в}\right)^2 + \left(\frac{N\lambda}{2\pi 8{,}68}\right)^2, \quad (1)$$

$$\operatorname{tg}\delta = \frac{(\Delta d\lambda_в + 2\Delta X\lambda) N\lambda}{\varepsilon' \pi 8{,}68\, \Delta d\lambda_в}, \quad (2)$$

where λ is wavelength in free space; $\lambda_{waveguide}$ is the wavelength in the waveguide; Δ d is change in sample thickness; ΔX, Δ T are the changes in X and T corresponding to the value Δ d; N = $\Delta T/\Delta d$ is specific absorption.

For samples with a sharply expressed inhomogeneity of the properties of ice in the thickness, for example, with a layered change in density and salinity, the constructed dependences X = f(d) and T = φ(d) differ from linear. In the sea ice cover such changes are especially clearly expressed in its upper part (snow with a density changing in the thickness of the layer, layer of ice breccia, water-snow

* V. V. Bogorodskiy, P. G. Zayets, G. K. Pogodin and G. P. Khokhlov, "Apparatus for Measuring the Electrical Parameters of Saline Ice at a Wavelength of 3 cm," in this collection of articles.

APPROVED FOR RELEASE: 2007/02/09: CIA-RDP82-00850R000500020040-0

APPROVED FOR RELEASE: 2007/02/09: CIA-RDP82-00850R000500020040-0

layer). In the lower part of the ice cover, as in its upper part, it is possible to observe a substantial change in ice salinity without sharply expressed changes in the structural and textural criteria. Figure 1 shows the possible changes in the X and T values as a function of sample thickness. The mean values ε' and $\operatorname{tg}\delta$ of all three samples are arbitrarily assumed to be equal and can be determined from expressions (1) and (2). Depending on from what layer the thickness of the sample decreases, for one and the same inhomogeneous sample there will be curves of different types (curves 2 or 3 in Fig. 1).

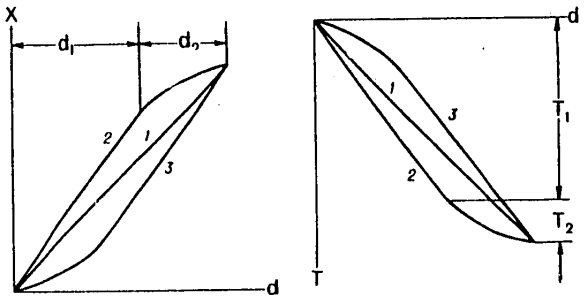

Fig. 1. Dependence of displacement X of minimum of standing wave and attenuation T on thickness of homogeneous (1) and inhomogeneous (2, 3) samples (2 -- increase in refractive index and specific absorption of ice with decrease in thickness of two-layer sample; 3) decrease in these parameters with increase in ice thickness).

In the case of a multilayer sample the computation of specific absorption of each layer involves no difficulties. Since $T = T_1 = T_2$ it is possible to find the mean specific absorption (N) and N for each layer for the sample

$$N = \frac{T}{d_1 + d_2}; \quad N_1 = \frac{T_1}{d_1}; \quad N_2 = \frac{T_2}{d_2}. \tag{3}$$

The interpretation of the dependence of X on the thickness of a multilayer sample is more complex since the ε' value for the entire sample does not conform to the additivity rule. In an investigation of such nonlinear dependences for computation of ε' it is necessary to approximate the curves 2 or 3 (see Fig. 1) by a series of straight lines and represent the sample in the form of a group of capacitors connected in series with losses. If one layer of the sample is characterized by the parameters C_1, R_1, and the other by the parameters C_2, R_2, by equating the impedance of the circuit to the resistance of an equivalent circuit (with the parameters C and R) it is possible to obtain the following expressions:

$$\frac{R_1}{1 + \omega^2 R_1^2 C_1^2} + \frac{R_2}{1 + \omega^2 R_2^2 C_2^2} = \frac{R}{1 + \omega^2 R^2 C^2}, \tag{4}$$

$$\frac{R_1^2 C_1}{1 + \omega^2 R_1^2 C_1^2} + \frac{R_2^2 C_2}{1 + \omega^2 R_2^2 C_2^2} = \frac{R^2 C}{1 + \omega^2 R^2 C^2}. \tag{5}$$

APPROVED FOR RELEASE: 2007/02/09: CIA-RDP82-00850R000500020040-0

APPROVED FOR RELEASE: 2007/02/09: CIA-RDP82-00850R000500020040-0

Substituting into expressions (4) and (5) the values

$$R_i = \frac{1}{\omega C_i \operatorname{tg}\delta_i} = \frac{4\pi d_i}{\omega \varepsilon_i' S \operatorname{tg}\delta_i},$$

$$R_i^2 C_i = \frac{4\pi d_i}{\omega^2 \varepsilon_i' S \operatorname{tg}^2 \delta_i},$$

(where i = 1, 2, 3; S is the area of the capacitor plates), and also introducing abbreviations on both sides of the equations, we obtain

$$\frac{d_2 \operatorname{tg}\delta_2}{\varepsilon_2'(1+\operatorname{tg}^2\delta_2)} = \frac{d \operatorname{tg}\delta}{\varepsilon'(1+\operatorname{tg}^2\delta)} - \frac{d_1 \operatorname{tg}\delta_1}{\varepsilon_1'(1+\operatorname{tg}^2\delta_1)}, \tag{6}$$

$$\frac{d_2}{\varepsilon_2'(1+\operatorname{tg}^2\delta_2)} = \frac{d}{\varepsilon'(1+\operatorname{tg}^2\delta)} - \frac{d_1}{\varepsilon_1'(1+\operatorname{tg}^2\delta_1)}. \tag{7}$$

After dividing the left- and right-hand sides of expressions (6) and (7) by one another, we obtain a final expression for $\operatorname{tg}\delta_2$

$$\operatorname{tg}\delta_2 = \frac{d\varepsilon_1' \operatorname{tg}\delta(1+\operatorname{tg}^2\delta_1) - d_1\varepsilon' \operatorname{tg}\delta_1(1+\operatorname{tg}^2\delta)}{d\varepsilon_1'(1+\operatorname{tg}^2\delta_1) - d_1\varepsilon'(1+\operatorname{tg}^2\delta)}, \tag{8}$$

and from equation (7) we obtain a final expression for ε'_2

$$\varepsilon_2' = \frac{\varepsilon'\varepsilon_1'(1+\operatorname{tg}^2\delta)(1+\operatorname{tg}^2\delta_1)d_2}{[d\varepsilon_1'(1+\operatorname{tg}^2\delta_1) - d_1\varepsilon'(1+\operatorname{tg}^2\delta)](1+\operatorname{tg}^2\delta_2)}. \tag{9}$$

When $\operatorname{tg}\delta_1 \ll 1$ formulas (8) and (9) are simplified

$$\operatorname{tg}\delta_2 = \frac{d\varepsilon_1' \operatorname{tg}\delta - d_1\varepsilon' \operatorname{tg}\delta_1}{d\varepsilon_1' - d_1\varepsilon'}, \tag{10}$$

$$\varepsilon_2' = \frac{\varepsilon'\varepsilon_1' d_2}{d\varepsilon_1' - d_1\varepsilon'}. \tag{11}$$

In an example we will demonstrate the process of computation of the electric parameters of the layers of an inhomogeneous sample extracted from the upper part of white ice. The measurements were made in a marginal part of the Bering Sea at an air temperature -8°C. The mean salinity of the sample was 2.68°/oo; it consisted of an unconsolidated layer of white ice with large bubbles with a thickness of 13 cm, undergoing an abrupt transition into a transparent dense layer of ice with a thickness 6 cm. The working of the sample for the purpose of reducing its thickness was from the direction of the unconsolidated layer. The curves constructed on the basis of experimental points (Fig. 2) are approximated by the straight lines 2 and 3. First using the straight lines 1 and 2 we find the mean value for the sample N_1 = 0.71 db/cm and the value N_2 = 1.35 db/cm for a layer of dense ice. Then we compute the refractive indices n_1 = 1.576, n_2 = 1.742, and taking into account the conditions of smallness of the attenuation factor k (N 3.23 db/cm) -- the relative dielectric constants $\varepsilon'_1 = n_1^2 = 2.48$; $\varepsilon'_2 = n_2^2 = 3.04$. Using expression (9)

APPROVED FOR RELEASE: 2007/02/09: CIA-RDP82-00850R000500020040-0

APPROVED FOR RELEASE: 2007/02/09: CIA-RDP82-00850R000500020040-0

we determine $\varepsilon'_3 = 2.3$ and $n_3 = \sqrt{\varepsilon'_3} = 1.52$. Taking into account that $k = N\lambda/2\pi \cdot 8.68$, and $\operatorname{tg}\delta = 2nk/\varepsilon'$, it is possible to find

$$k_1 = 3{,}89 \cdot 10^{-2},$$
$$k_2 = 7{,}4 \cdot 10^{-2},$$
$$\operatorname{tg}\delta_1 = 4{,}94 \cdot 10^{-2},$$
$$\operatorname{tg}\delta_2 = 8{,}5 \cdot 10^{-2}.$$

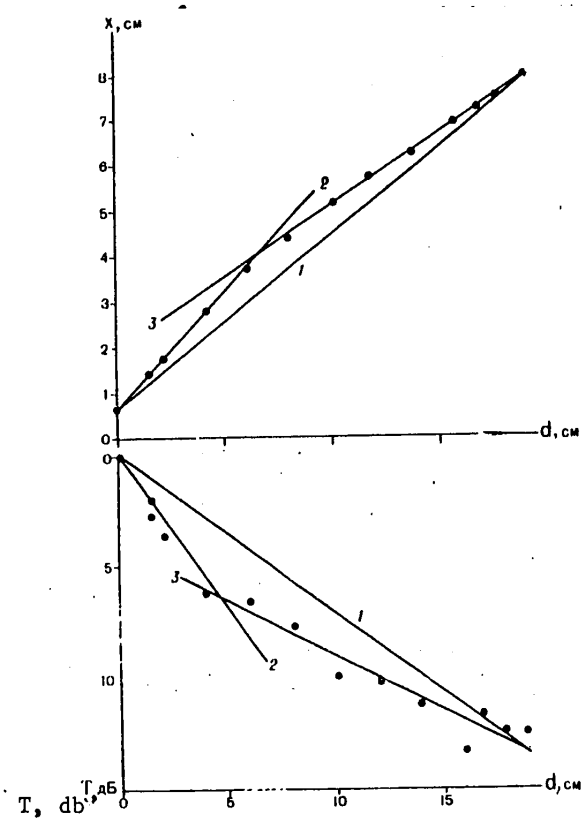

Fig. 2. Experimental nonlinear dependences for sample extracted from upper part of sea ice cover. 1) straight line for computing mean values of ice parameters; 2, 3) approximating straight lines for layers with greater and lesser N and n values respectively.

Using expression (8) we determine $\operatorname{tg}\delta_3 = 3.72 \cdot 10^{-2}$. The value $N_3 = 0.515$ db/cm, computed from the parameters ε'_3 and $\operatorname{tg}\delta_3$, differs by not more than 3% from the value $N_3 = 0.5$ db/cm, found graphically using expressions (3). In this study we have derived equations and outlined a method for computing the parameters of a two-layer sample as being the most typical in studies of the electrical properties of sea ice. It is easy to make similar studies for multilayer samples.

COPYRIGHT: Arkticheskiy i antarkticheskiy nauchno-issledovatel'skiy institut (AANII), 1975

APPROVED FOR RELEASE: 2007/02/09: CIA-RDP82-00850R000500020040-0

APPROVED FOR RELEASE: 2007/02/09: CIA-RDP82-00850R000500020040-0

APPARATUS FOR MEASURING THE ELECTRICAL PARAMETERS OF SALINE ICE AT λ3 cm

Leningrad TRUDY. ORDENA LENINA ARKTICHESKIY I ANTARKTICHESKIY NAUCHNO-ISSLEDOVATEL'-SKIY INSTITUT. RADIOFIZICHESKIYE METODY ISSLEDOVANIY VODNYKH MASS SNEGA I L'DA
in Russian No 324, 1974 pp 50-56

[Article by V. V. Bogorodskiy, P. G. Zayets, G. K. Pogodin and G. P. Khokhlov]

[Text] In selecting a method for measuring the parameters of saline ice in the SHF range it is necessary that two principal factors be taken into account: the possibility of the existence of large ice crystals and large inhomogeneities in the natural ice cover and also the presence therein of a liquid phase and salts causing a considerable absorption of electromagnetic energy. The first factor requires the fabrication of such a measurement apparatus as will make it possible to obtain information on the averaged electric parameters of a sufficiently great volume of inhomogeneous sea ice. Apparatus in which the measurement element used is segments of waveguides filled with ice [3, 4] only in the first approximation must be regarded as suitable for investigations of natural ice. Information on the parameters of ice of a considerable volume can be obtained by using optical measurement methods [1, 2]. The second factor determines the requirements on the technical possibilities of the apparatus, that is, on its response, accuracy and energy potential. In addition, due to the great absorption of electromagnetic energy there is no possibility for carrying out in situ measurements of the mean electrical parameters of the entire thickness of the ice cover. Accordingly, samples of ice of sufficiently large size should be used in the measurement apparatus as the object to be measured, taking into account the enumerated requirements.

In this article we give a description of an apparatus for measuring the refractive index and the specific absorption of ice at a wavelength of 3 cm based on the optical method for measuring the complex coefficient of transparency of samples in free space and constructed using a high-response balanced circuit.

We will examine the incidence of an electromagnetic wave with the amplitude $A_1 = 1$ from the air (medium 1) on a sample (medium 2) of ice with the thickness d. Assume that the measured parameters will be the modulus and phase of a wave propagating into the air (medium 3) through the sample, that is

$$A_3 = |A_3| e^{j\varphi_3}.$$

The components E and H for each medium can be written in the form

APPROVED FOR RELEASE: 2007/02/09: CIA-RDP82-00850R000500020040-0

APPROVED FOR RELEASE: 2007/02/09: CIA-RDP82-00850R000500020040-0

$$\left.\begin{aligned} E_1 &= e^{jk_0x} + B_1e^{-jk_0x} \\ H_1 &= y\left(e^{jk_0x} - B_1e^{-jk_0x}\right) \end{aligned}\right\} \quad (1)$$

$$\left.\begin{aligned} E_2 &= A_2e^{jk_0\dot{n}x} + B_2e^{jk_0\dot{n}x} \\ H_2 &= y\dot{n}\left(A_2e^{jk_0\dot{n}x} - B_2e^{-jk_0\dot{n}x}\right) \end{aligned}\right\} \quad (2)$$

$$\left.\begin{aligned} E_3 &= A_3e^{jk_0x} \\ H_3 &= yA_3e^{jk_0x}, \end{aligned}\right\} \quad (3)$$

where $k_0 = 2\pi/\lambda$ is the wave number; A_1, B_1 are the amplitudes of the incident and reflected waves in the i-th medium; x is a coordinate in the direction of propagation; y is the conductivity of media 1 and 3; $\dot{n}$ is the complex refractive index of medium 2.

Using equations (1-3) with x = 0 (the boundary of media 1 and 2) and with x = d it is possible to obtain a fundamental expression in which the modulus and the phase of a wave propagating through medium 2 are related to the complex refractive index of this medium,

$$\frac{4}{A_3}e^{jk_0d} = \frac{(\dot{n}+1)^2e^{-jk_0\dot{n}d} - (\dot{n}-1)^2e^{jk_0\dot{n}d}}{\dot{n}}. \quad (4)$$

Substituting into expression (4) the value

$$\dot{n} = n - jk,$$

(where n is the refractive index; k is the absorption coefficient), and also representing expression (4) in the form

$$\frac{4}{A_3}e^{-jk_0d} = C_1 - jC_2 = |C|e^{j\varphi}, \quad (5)$$

we find

$$C_1 = \left|\left(n + \frac{n}{n^2+k^2}\right)\left(\frac{1}{\gamma} - \gamma\right) + 2\left(\frac{1}{\gamma} + \gamma\right)\right|\cos\psi - \left|\left(k - \frac{k}{n^2+k^2}\right)\left(\frac{1}{\gamma} + \gamma\right)\right|\sin\psi; \quad (6)$$

$$C_2 = \left|\left(n + \frac{n}{n^2+k^2}\right)\left(\frac{1}{\gamma} + \gamma\right) + 2\left(\frac{1}{\gamma} - \gamma\right)\right|\sin\psi + \left|\left(k - \frac{k}{n^2+k^2}\right)\left(\frac{1}{\gamma} - \gamma\right)\right|\cos\psi, \quad (7)$$

where

$$\gamma = e^{k_0dk}; \quad \psi = k_0dn.$$

We will examine the case of strong attenuation of waves in the sample when $\gamma \gg 1$ and we will neglect the value $1/\gamma \gg \gamma$. Then expressions (6) and (7) can be represented in the form

$$C_1 = \alpha\cos\psi + \beta\sin\psi;$$

$$C_2 = \alpha\sin\psi + \beta\cos\psi,$$

where

$$\alpha = \gamma\left|\left(n + \frac{n}{n^2+k^2}\right) - 2\right|; \quad \beta = \gamma\left(k - \frac{k}{n^2+k^2}\right).$$

APPROVED FOR RELEASE: 2007/02/09: CIA-RDP82-00850R000500020040-0

APPROVED FOR RELEASE: 2007/02/09: CIA-RDP82-00850R000500020040-0

Since $$|C|^2 = C_1^2 + C_2^2 = \alpha^2 + \beta^2,$$

and the modulus of the left-hand side of expression (6) is

$$\left| \frac{4}{A_3} e^{-jk_0 d} \right|^2 = \frac{4}{A_3} e^{-jk_0 d} \frac{4}{A_3^*} e^{jk_0 d} = \frac{4}{|A_3|^2},$$

we will determine

$$|A_3|^2 = \frac{4}{\alpha^2 + \beta^2}.$$

The latter expression indicates the absence of oscillations caused by rereflections from the walls of the sample in the case of adequately great attenuation of electromagnetic energy.

We will examine the change in phase φ with a change in the thickness of the sample and the related ψ value. Since

$$C_2 / |C| = \sin\varphi, \text{ a } |C| = \sqrt{\alpha^2 + \beta^2},$$

$$\varphi = \arcsin \frac{C_2}{|C|} = \arcsin \frac{-\alpha \sin\psi + \beta\cos\varphi}{\sqrt{\alpha^2 + \beta^2}}.$$

We introduce as a convenience the annotations

$$\frac{\alpha}{\sqrt{\alpha^2 + \beta^2}} = \cos\varphi_0, \quad \frac{\beta}{\sqrt{\alpha^2 + \beta^2}} = \sin\varphi_0.$$

Then

$$\varphi = \arcsin(-\cos\varphi_0 \sin\psi + \sin\varphi_0 \cos\psi) = \varphi_0 + \psi.$$

Since φ_0 is evidence of the initial constant phase shift, determined by α and β, and accordingly, n and k, the phase change is dependent only on the change in ψ: $\Delta\varphi = \Delta\psi$ or $\Delta\varphi = k_0 \Delta dn$. Hence we see that there is a linear dependence of the phase change on the thickness of the sample, having a strong absorption.

It is possible to determine under what conditions oscillations of the transparency coefficient will be absent. Oscillations will evidently be absent if the amplitude of the first rereflected wave, propagating into the medium 3, is considerably less than the amplitude of the direct wave in this medium, that is

$$e^{-k_0 2dk} \ll 1.$$

This condition is observed when $k_0 2dk > 2$ and it therefore follows that

$$k \gg \frac{\lambda_0}{2\pi d}. \qquad (8)$$

The measurement apparatus consists of the waveguide elements and units shown in Fig. 1.

The amplitude-modulated signal received from the generator is divided into two parts. Part of the SHF energy is radiated into the space between the horns where the sample 6 can be placed. Another part of the energy, playing the role of a reference

APPROVED FOR RELEASE: 2007/02/09: CIA-RDP82-00850R000500020040-0

APPROVED FOR RELEASE: 2007/02/09: CIA-RDP82-00850R000500020040-0

signal, is directed through the uncalibrated attenuator 7, serving for compensation of the total energy losses in the upper part of the system (see Fig. 1) in the measurement elements 8 and 9. The reference signal and the signal arriving from the receiving antenna, interfering with one another, give a standing wave which is registered by the measurement line sonde. The signal arriving from the measurement line sonde is amplified by an amplifier and is observed on an oscilloscope screen. After introducing the ice sample between the horns the wave phase shift is determined by the displacement of the standing wave minimum in the measurement line. Attenuation is determined by the difference between the new and former readings of the precise measurement attenuator.

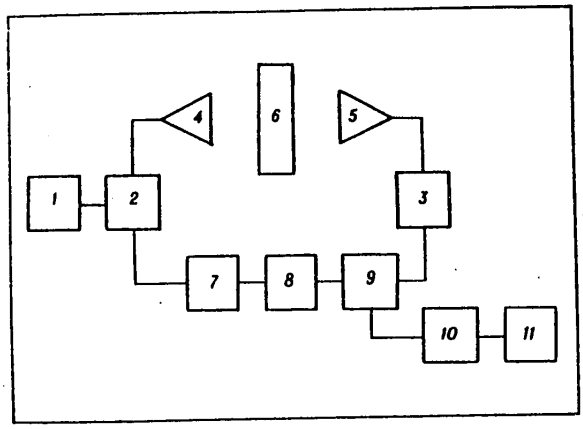

Fig. 1. Block diagram of measurement apparatus. 1) GZ-26 signal generator; 2, 3) directional couplers; 4, 5) transmitting and receiving horn antennas; 6) sample; 7) uncalibrated compensating attenuator; 8) D5-33 measurement attenuator; 9) R1-4 waveguide measurement line; 10) U2-4 amplifier; 11) S1-5 oscilloscope.

Since all the apparatus elements are fixed in position, it is somewhat more convenient than an apparatus in which the phase change after introduction of the sample between the horns is determined by the displacement of the horn [1].

Since in the apparatus employed the displacement of the standing wave minimum is registered in the measurement line waveguide, and the movement of the sonde in this case occurs simultaneously relative to the reference signal and the signal propagating through the sample, the expression for the refractive index under the condition of strong attenuation assumes the form

[B = waveguide]

$$n = 1 + \frac{2X}{d} \cdot \frac{\lambda}{\lambda_в},$$

where X is the displacement of the standing wave minimum in the measurement line; $\lambda_{\text{waveguide}}$ is the wavelength in the waveguide.

APPROVED FOR RELEASE: 2007/02/09: CIA-RDP82-00850R000500020040-0

APPROVED FOR RELEASE: 2007/02/09: CIA-RDP82-00850R000500020040-0

Thus, the refractive index is determined by the slope of the straight line on the graph of the dependence of measurement line readings on ice thickness

[B = waveguide]
$$n = 1 + \frac{2\Delta X}{\Delta d} \cdot \frac{\lambda}{\lambda_в}, \quad (9)$$

where ΔX is the change in the X value with a change in thickness by Δd.

Specific absorption in the ice is determined by the slope on the graph of the dependence of signal attenuation on sample thickness

$$N = -\frac{\Delta T}{\Delta d}, \quad (10)$$

where ΔT is the change in attenuation T with a change in thickness by Δd.

At the same time, specific absorption is related to the absorption coefficient by the expression

$$N = 8{,}68 \frac{2\pi}{\lambda} k. \quad (11)$$

In addition, it is known that

$$\varepsilon' = n^2 - k^2. \quad (12)$$

Thus, using the measured values it is possible to compute any electric parameters of the ice.

A test of the correctness of computation of n is unambiguity in determining the minimum points in the measurement line with a change in sample thickness, reflecting the truth of the slope of the straight line X = f(d). Such an unambiguity is realized only in a case when the change in thickness by the value Δd causes a displacement of the minimum in the range $\Delta X = \lambda_{waveguide}/2$ (in this case $\Delta X = 2$ cm). It follows from expression (9) that for fresh ice with n = 1.775 Δd should be not greater than 3.87 cm, whereas for sea ice with a possible anticipated value n = 3 Δd should not exceed 1.35 cm. Thus, always selecting Δd at about 1 cm, it is possible to guarantee unambiguity in determining the phase shift caused by a change in the thickness of the sample, and accordingly, unambiguity in determining n within the limits of the indicated changes in its values.

Figure 2 shows the dependence of X and T on the thickness of three identical samples extracted in the marginal part of the Bering Sea from a plate of gray ice. The measurements were made at a temperature -9°C. Sample salinity was 6.62°/oo. The results of the measurements coincide with an accuracy to ±1% for n and with an accuracy to ±10% for N. The refractive index of ice and specific absorption, computed from the straight lines in Fig. 2, are equal to 1.87 and 1.69 db/cm respectively. For one of the samples, whose thickness varied each 5 mm, in the dependence T = f(d) it is possible to trace a periodicity with a wavelength of 4 cm and an amplitude of about 1 db. This periodicity is related to reflections in waveguide channels and horn antenna systems which are difficult to take into account. It is evident that the periodicity, if it is detected on the graph by means of measurement of sample thickness with a small discreteness, exerts no influence on the accuracy in measuring specific absorption, which is determined, as follows from

APPROVED FOR RELEASE: 2007/02/09: CIA-RDP82-00850R000500020040-0

APPROVED FOR RELEASE: 2007/02/09: CIA-RDP82-00850R000500020040-0

expression (10), by the accuracy in measuring ΔT and Δd (about 10%).

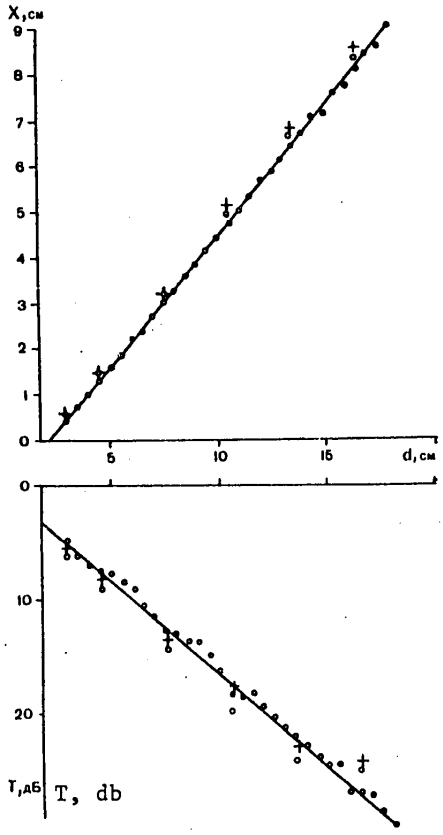

Fig. 2. Dependence of parameters X and T on thickness of samples d. Three types of points correspond to the results of measurements of three samples.

However, if the sample thickness is decreased by a Δd value greater than a quarter of the period of the oscillating curve, greater errors can arise in determining specific absorption. In this case the relative error can be computed from the expression

$$\delta = \pm \frac{1}{N_{true} d} \cdot 100\%, \qquad (13)$$

where N_{true} is the true specific absorption.

It can be seen from formula (13) that the error decreases with an increase in sample thickness and N_{true}. It is possible to estimate the possible errors which may appear in such measurements. With a value $N_{true} d$ = 30 db (an attenuation at which the signal minimum was registered quite reliably) δ does not exceed ±3%. With small specific absorptions (N_{true} about 0.5 db/cm) and a sample thickness of about

APPROVED FOR RELEASE: 2007/02/09: CIA-RDP82-00850R000500020040-0

APPROVED FOR RELEASE: 2007/02/09: CIA-RDP82-00850R000500020040-0

20 cm the error is greater but not greater than ±10%. Taking into account that the accuracy in reading on the measurement line rule is 0.01 mm, and the parallelism of the sample surfaces when processed on a special coordinate instrument does not exceed 1 mm, the relative error in determining the refractive index attains ±1%.

It is possible to estimate the specific absorption value for which the error in determining ε' from expression (12) will not exceed a given value, such as 1%. With $\varepsilon' = 3.15$, if $k^2 = 0.0315$, $k = 0.177$, it follows from formula (11) that $N \leqslant 3.23$ db/cm.

It is necessary to mention a favorable factor exerting an influence on the accuracy in computing ε'. In the case of large N_{true} values, as can be seen from expression (13), the error in computing spectific absorption, and accordingly k, is small. Therefore ε' is computed with sufficient accuracy. With small N_{true} values the k^2 value is small and therefore its influence on the dielectric constant in some cases can be neglected.

This measurement apparatus was used in determining the electric parameters of sea ice during the Soviet-American "Bering" experiment. Similar apparatus can be fabricated for investigations at other frequencies in the centimeter range and be used not only for measuring the parameters of ice, but also the characteristics of other materials with strong absorption.

BIBLIOGRAPHY

1. Brand, A. A., ISSLEDOVANIYE DIELEKTRIKOV NA SVERKHVYSOKIKH CHASTOTAKH (Investigation of Dielectrics at Superhigh Frequencies), Moscow, Gos. Izd-vo Fiz.-Mat. Lit-ry, 1963, 403 pages.

2. Starikov, V. D., METODY ISSLEDOVANIYA NA SVCh S PRIMENENIYEM IZMERITEL'NYKH LINIY (Methods for SHF Investigations With Use of Measurement Lines), Moscow, "Sovetskoye Radio," 1972, 144 pages.

3. Hoekstra, P., "The Dielectric Properties of Sea Ice at UHF and Microwave Frequencies," PROCEEDINGS OF THE INTERNATIONAL MEETING ON RADIOGLACIOLOGY, pp 32-53, 1970.

4. Cumming, W. A., "The Dielectric Properties of Ice and Snow at 3.2 cm," J. APPL. PHYS., Vol 23, No 7, pp 768-773, 1952.

COPYRIGHT: Arkticheskiy i antarkticheskiy nauchno-issledovatel'skiy institut (AANII), 1975

APPROVED FOR RELEASE: 2007/02/09: CIA-RDP82-00850R000500020040-0

APPROVED FOR RELEASE: 2007/02/09: CIA-RDP82-00850R000500020040-0

REGISTRY OF ACOUSTIC WAVES TRANSMITTED FROM WATER INTO ICE

Leningrad TRUDY. ORDENA LENINA ARKTICHESKIY I ANTARKTICHESKIY NAUCHNO-ISSLEDOVATEL'-SKIY INSTITUT. RADIOFIZICHESKIYE METODY ISSLEDOVANIY VODNYKH MASS SNEGA I L'DA in Russian No 324, 1974 pp 104-108

[Article by I. K. Popov]

[Text] In the practice of use of acoustic methods and apparatus in investigations of ocean areas covered by ice in many cases it is necessary to employ hydroacoustic converters embedded in the ice for the reception of acoustic oscillations from the water medium. Such a necessity arises, for example, when measuring the depth of water bodies through the ice cover or in the registry of seismoacoustic noise from sources situated at a considerable distance from the reception point when the waves, propagating directly into the ice in the acoustic frequency range, attenuate.

Such investigations have demonstrated that acoustic converters, which in a water medium within the limits of the acoustic frequency range are nondirectional, when embedded in the ice exhibit directional properties relative to the oscillations arriving from the water medium. An analysis of this phenomenon indicates that this can be attributed to the conditions for sound propagation under the ice and the acoustic characteristics of transition of sound from water into ice; the latter factor, having an angular dependence, plays the decisive role. In addition, depending on the frequency of the registered oscillations, the ice cover plays the role of a sort of plate, a layer of finite thickness or a semi-infinite medium.

In the central part of the Arctic basin, the thickness of the perennial ice on which most of the seismoacoustic investigations are made from the drifting stations averages 3 m. Such ice can be considered a thin plate with elastic oscillations having frequencies not greater than 20-30 Hz, that is, in the subsonic region.

At these frequencies for a plate lying on an elastic half-space flexure is the only possible type of deformation. With such a representation of the ice cover its influence on the nature of reflection of elastic waves arriving from the water medium is manifested as a second-order effect [1]: the reflection coefficient for a plane wave in absolute value is close to unity and its phase differs little from the π value which it would have in the case of a free surface of the fluid.

In such situations it is possible to regard an acoustic detector embedded in the ice as a converter situated within an infinite screen. The influence of an ice layer situated between the converter and water at low frequencies, as a result of

APPROVED FOR RELEASE: 2007/02/09: CIA-RDP82-00850R000500020040-0

APPROVED FOR RELEASE: 2007/02/09: CIA-RDP82-00850R000500020040-0

small attenuation, can be neglected. The directivity characteristics of the converter operating in an infinite screen is determined by the following expression:

$$R_{\theta} = \frac{2I_1\left(\frac{\pi d}{\lambda}\sin\theta\right)}{\frac{\pi d}{\lambda}\sin\theta}, \quad (1)$$

$2I_1$ is a Bessel function of the first kind, of the first order; d is the diameter of the converter.

The directivity of such a system begins to be reflected at frequencies corresponding to the expression $d/\lambda = 1/2$.

Taking into account the real dimensions of the used converters (~150 mm) their directivity begins to be manifested from a frequency of about 5 KHz. Thus, in the subsonic region the converters embedded in the ice are virtually nondirectional. With an increase in the frequency of the registered oscillations of the ice cover the latter no longer can be regarded as a thin plate. In addition, with an increase in frequency there is an increase in the attenuation of sound in the ice. As a result, at frequencies of about 1 KHz and above the ice for all practical purposes can be regarded as a semi-infinite medium. In order to obtain the energy ratios for the transition of acoustic waves from the fluid to the solid medium the author of [3] introduces the concept of input resistance of the solid medium with the incidence of a plane wave of a fluid on it at the arbitrary angle θ_0. It is expressed by the following relationship:

[T = solid]

$$z_r = z\cos^2 2\vartheta + \xi\sin^2 2\vartheta, \quad (2)$$

where $z = \rho c_d/\cos\theta$, $\xi = \rho c_r/\cos\vartheta$ are the wave resistances of the solid medium for longitudinal and transverse waves respectively; c_d, c_r are the velocities of longitudinal and transverse waves; θ and ϑ are the refraction angles for longitudinal and transverse waves with an angle of incidence from the fluid θ_0.

Expression (2) is reduced to the form

$$z_r = \frac{\rho c_d}{\cos\theta} k_r,$$

$$k_r = 1 - \sin^2 2\vartheta\left(1 - \frac{\operatorname{tg}\vartheta}{\operatorname{tg}\theta}\right). \quad (3)$$

It follows from formula (3) that the angular characteristic of the input resistance of the solid medium is dependent only on the "stiffness" of the solid medium and in the limits of the angles $\sin\theta \leqslant 0.9$, that is, the value of the angle of total internal reflection for longitudinal waves remains almost constant since the increase in z_{solid} due to a decrease in $\cos\theta$ in the denominator is compensated by approximately the same decrease in the k_{solid} coefficient. The sharp dropoff in the input resistance is attributable to the fact that the correction

$$\sin^2 2\vartheta\left(1 - \frac{\operatorname{tg}\vartheta}{\operatorname{tg}\theta}\right)$$

is dictated by the effect of shear waves, has a maximum at $\sin\theta \simeq 0.8$, after which it decreases rapidly.

APPROVED FOR RELEASE: 2007/02/09: CIA-RDP82-00850R000500020040-0

APPROVED FOR RELEASE: 2007/02/09: CIA-RDP82-00850R000500020040-0

Thus, the input resistance of the ice cover for longitudinal and transverse waves remains virtually unchanged up to the angle of total internal reflection for longitudinal waves, after which it sharply increases. The angle of incidence θ_0 at which the total internal reflection of longitudinal waves for ice is observed according to computations is 30-32°, depending on the properties of the ice associated with its formation. Accordingly, a detector embedded in the ice seemingly has a directivity characteristic having an aperture angle of approximately 60-65° relative to the signals arriving from the water. On the other hand, source [2] gives computed data on the angular dependence of the coefficient of reflection of sound from the water-ice discontinuity for ice with values of the velocity of elastic waves in the ice from $2 \cdot 10^5$ to $3.7 \cdot 10^5$ cm/sec. These show that the coefficient of reflection at the water-ice discontinuity becomes close to 1 with angles of incidence from 22-40 to 90°, dependent on the elastic properties of the ice and its density. It follows from these data that the directivity of the embedded detectors is 45-90°.

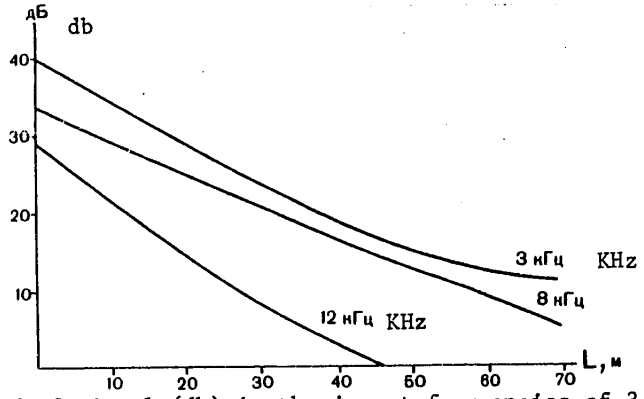

Fig. 1. Dropoff of signal (db) in the ice at frequencies of 3, 8, 12 KHz with horizontal movement of sound source at a depth of 10 m.

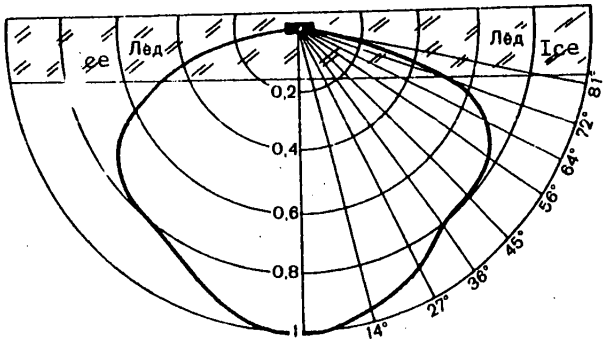

Fig. 2. Directivity (in degrees) of detector embedded in ice relative to oscillations transmitted into ice from water.

At frequencies of the order of tens and hundreds of Hz the ice cover plays the role of a layer of finite thickness with the transmission of acoustic waves into it from the water medium. The wave pattern in this case is considerably complicated. Taking into account the insignificant attenuation of sound in the ice at these frequencies, it can be postulated that during the reception of signals in the ice

APPROVED FOR RELEASE: 2007/02/09: CIA-RDP82-00850R000500020040-0

APPROVED FOR RELEASE: 2007/02/09: CIA-RDP82-00850R000500020040-0

standing waves will develop in its thickness with a distribution of amplitudes changing with frequency. In this case in the reception of oscillations from the water the depth to which the detector is embedded in the thickness of the ice cover can be extremely important. In this case it is entirely possible that it is desirable that the detector not be embedded in the ice but that it be placed, for example, in a vertical opening made in the ice and filled with a nonfreezing solution and by its movement in this opening a maximum value of the amplitude of the received oscillations be achieved.

The experimental checking of the conditions for the reception of oscillations from the water by detectors embedded in the ice was carried out at the "Severnyy Polyus-15" drifting station simultaneously with study of sound attenuation in ice. A detector embedded in the ice to a depth of about 1 m registered signals from a sound source placed first in the ice layer and then in the water. The sound source present in the water moved in the horizontal plane at a depth of 10 m at the lower surface of ice, whose thickness at the observation point was 2.8 m. The signals from the sound source were registered simultaneously by a detector embedded in the ice and a detector situated in the water directly under the lower surface of the ice and on the same vertical with the first. The sound source was moved horizontally for a distance up to 150 m from the site of the detectors. Curves of the dropoff of signals registered by both detectors made it possible to determine the angular dependence of the levels registered by the detector in the ice (Fig. 1).

Figure 2 shows the computed (on the basis of experimental data) angular characteristic of response for a detector in the ice at a frequency of 3 KHz, taking into account the dropoff of the signal in the water due to divergence of the wave front in conformity to a spherical law. The directivity characteristic at a frequency of 8 KHz, judging from the curves of signal dropoff, differs little from that cited in Fig. 2, but at a frequency of 12 KHz the angle characterizing the directivity will be somewhat more acute.

Thus, the experimental results indicate that the directivity of an acoustic detector embedded in the ice has a broader maximum than follows from the computed data. The angle of aperture of this characteristic at a frequency of several KHz is 125-140°. This is evidently attributable to the fact that in the computations no allowance was made for the unevenness of the lower ice surface, due to which the sound penetrates into the ice with angles of incidence greater than the computed values. It is known that in the case of propagation under the ice the energy of the acoustic field is concentrated in the near-ice water layer and the angles of emergence of rays experiencing total internal reflection are up to 10°. Accordingly, it must be expected that with detectors embedded in the ice it is difficult to register sources situated at distances greater than one cycle of the boundary ray, that is, at distances of more than ten kilometers, because the acoustic energy propagating along rays close to boundary rays and having the least attenuation with distance virtually does not penetrate into the ice.

BIBLIOGRAPHY

1. Krasil'nikov, V. I., RASPROSTRANENIYE IZGIBNYKH VOLN (Propagation of Flexural Waves), Report of Leningrad State University, 1960, 118 pages.

APPROVED FOR RELEASE: 2007/02/09: CIA-RDP82-00850R000500020040-0

APPROVED FOR RELEASE: 2007/02/09: CIA-RDP82-00850R000500020040-0

2. Stashkevich, A. P., AKUSTIKA MORYA (Marine Acoustics), Leningrad, "Sudostroyeniye," 1966, 356 pages.

3. Tartakovskiy, B. D., "Transmission of Acoustic Waves Through the Discontinuities of Solid and Liquid Media," ZHURNAL TEKHNICHESKOY FIZIKI (Journal of Technical Physics), Vol 21, No 10, pp 1199-1201, 1951.

COPYRIGHT: Arkticheskiy i antarkticheskiy nauchno-issledovatel'skiy institut (AANII), 1975

APPROVED FOR RELEASE: 2007/02/09: CIA-RDP82-00850R000500020040-0

APPROVED FOR RELEASE: 2007/02/09: CIA-RDP82-00850R000500020040-0

USE OF DOPPLER EFFECT IN LASERS FOR INVESTIGATING STRESSED STATE OF ICE

Leningrad TRUDY. ORDENA LENINA ARKTICHESKIY I ANTARKTICHESKIY NAUCHNO-ISSLEDOVATEL'-SKIY INSTITUT. RADIOFIZICHESKIYE METODY ISSLEDOVANIY VODNYKH MASS SNEGA I L'DA in Russian No 324, 1974 pp 114-117

[Article by V. V. Bogorodskiy, V. P. Gavrilo and I. P. Ivanov]

[Text] One of the highly promising methods for obtaining complete information on the stressed state of ice is based on the use of the Doppler effect in lasers. The merit of this method, in particular, is that it makes it possible to carry out continuous registry of the rates of relative movement of different points (sectors) of the ice cover and thereby determine the deformation and its temporal change. In comparison with others this method has a considerably greater dynamic range, a better resolution, and makes it possible to register the rate of change of deformation from values of about 1μm/sec or more.

In this article we examine some results of testing of a method for experimental determination of dynamic stresses in the ice using a Doppler laser system. The experiment was carried out on the ice of Lake Ladoga in April 1972. The thickness of the ice was 70 cm; the air temperature was from -2 to -3°C. The idea of the experiment for determining deformation of the ice cover and its temporal changes involved measurement of the difference frequency of the beats arising as a result of interaction of the radiation reflected from the moving object and the direct laser radiation.

The principal element of the measuring apparatus was a laser (type OKG-13) whose divergence angle was $1.2 \cdot 10^{-3}$ rad. The radiation from one of the ends of the laser was directed on a mirror mounted at a distance of 0.5 m directly on the ice cover.

An FEU-36 photomultiplier was connected to the second end of the laser; it was sensitive to the radiation range 3000 A-6000 A. There was an interference filter at λ = 6328 A for eliminating background radiation having a transmission band 24 A. The light beats discriminated by the FEU were amplified by a wide-band amplifier and through a cathode repeater were registered by a loop oscillograph (type N-105). The reflection coefficient for the reflection mirror with a silver coating was 96%.

The entire apparatus operated as a laser deformograph in an ice sector 0.5 m. Without being inferior in response to seismic apparatus, the laser deformograph is a wider-band instrument which makes it possible to register aperiodic displacements

APPROVED FOR RELEASE: 2007/02/09: CIA-RDP82-00850R000500020040-0

APPROVED FOR RELEASE: 2007/02/09: CIA-RDP82-00850R000500020040-0

and oscillations of the ice cover in a very broad frequency range.

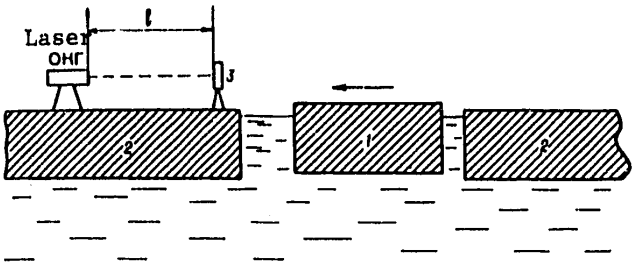

Fig. 1. Diagram of experiment for determining dynamic stresses in ice. 1) floe; 2) ice cover; 3) reflection mirror.

For our purposes the laser must operate in a single-frequency regime. There must be a brief frequency stability during the time of propagation of radiation to the reflector and back, that is, during the time $t = 300/3 \cdot 10^{10} = 10^{-8}$ sec. During this time the frequency must not change by more than 1% from the postulated Doppler shift, that is, 10^{-3} Hz.

The stresses in the measured sector l (Fig. 1) of the ice cover were created in the following way. In an ice hole (measuring 2 x 4 m) there was a floating floe which was brought into movement at different rates in the direction indicated by the arrow. With impact of the floe on the ice cover a stress and a corresponding deformation arise in it. On the oscillogram of the impact process and the phenomena accompanying it there was time scanning of the Doppler frequency, which was proportional to the rate of movement of the mirror and the laser, that is, to the temporal rate of deformation. Thus, if it is assumed that the ice under experimental conditions behaves as an elastic body, the stress in the ice can be estimated in the following way.

From the expression for the Doppler frequency Δf we determine the velocity v of ice particles with transmission of a voltage pulse caused by impact of the floe,

$$\Delta f = \frac{2v}{c} \nu;$$

$$v = \frac{\Delta f c}{2\nu} = \Delta f \frac{10^{10}}{2 \cdot 5{,}4 \cdot 10^{14}} = 2{,}9 \cdot 10^{-5} \Delta f,$$

where ν is the laser radiation frequency; c is the speed of light.

After processing the impact oscillogram we obtained a graph of the curve of change of Δf with time (Fig. 2). An analysis of the oscillogram reveals that initially our measurement system registers natural oscillations of the ice. The system reacts only to horizontal compressions and dilatations. Vertical displacements exert an influence only on the intensity of the light ray incident on the photodetector. Evidently, to some degree the registered signal could also be influenced by vibration of the connecting hoses between individual units of the measurement complex arising despite the measures undertaken for eliminating the influence of the wind on the entire system, which was situated partially on the ice and partially in the

APPROVED FOR RELEASE: 2007/02/09: CIA-RDP82-00850R000500020040-0

APPROVED FOR RELEASE: 2007/02/09: CIA-RDP82-00850R000500020040-0

laboratory. (The laboratory was a pavilion on runners with a height of about 2 m, which was at a distance of 1.5 m from the measurement base sector).

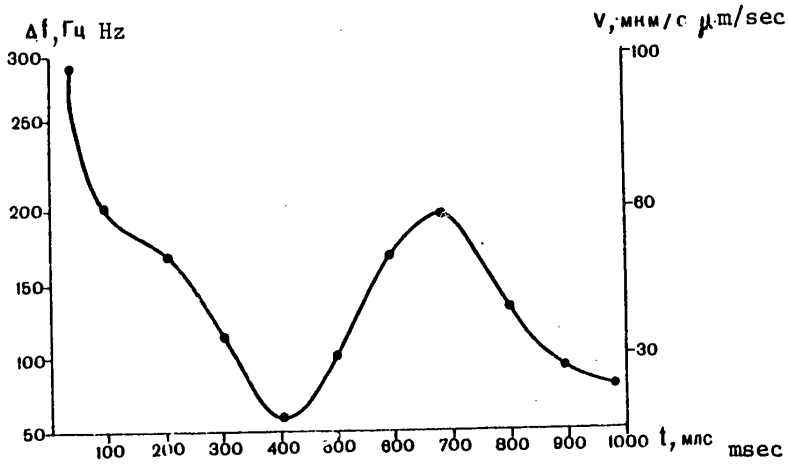

Fig. 2.Temporal change Δf (or change in v) according to results of processing of "impact oscillogram."

The rate at which the natural (background) displacements of ice particles occurs is approximately 2.5-20μ/sec. The corresponding frequencies of the natural oscillations of the ice cover are approximately 1-10 Hz. At the time t_0 of impact the velocity increases sharply and then changes in conformity to the curve (see Fig. 2).

Such a dependence of the rate of displacement indicates the following mechanism of propagation of an elastic wave in the ice. Initially the reflection mirror begins to move toward the laser. Then another wave reaches the laser and it, like the reflector, moves in one direction, as a result of which there is a subsequent decrease in velocity. Again the registered increase in the velocity indicates that the reflector begins to move in the opposite direction from the laser. The same nature of change in the relative velocity of movement of the ice particles in the measured sector with the length l was also observed on the remaining oscillograms of floe impacts.

We will determine the stress in the ice cover operative, for example, in the first $\Delta t = 0.05$ sec after the impact

$$v = 2.9 \cdot 10^{-5} \cdot 300 \approx 100 \mu m/sec.$$

The absolute change in a base with the length l is equal to

$$\Delta l = v \Delta t = 100 \cdot 0.05 = 5 \mu m.$$

APPROVED FOR RELEASE: 2007/02/09: CIA-RDP82-00850R000500020040-0

APPROVED FOR RELEASE: 2007/02/09: CIA-RDP82-00850R000500020040-0

The corresponding deformation ε of the measured base (l = 50 cm) in relative units (or percent) is

$$\varepsilon = \frac{\Delta l}{l} = 10^{-5}(0{,}01\%).$$

The Young modulus, evaluated from the velocity of propagation of longitudinal waves in the ice cover, is equal to

$$E = \rho c^2 \simeq 95 \text{ т/см}^2.$$

Then the stress will be

$$\sigma = \varepsilon E = 10^{-5} \cdot 95000 = 0{,}95 \text{ kg/cm}^2.$$

In evaluating the stresses in the ice in an impact produced by a different method from the measured values of the mass of the impact body, its velocity at the time of impact, the area of contact and impact time, it was possible to obtain comparable results differing from the computed value σ by about 0.5 kg/cm^2.

For a more correct approach to determination of stresses in the ice by the proposed method it is desirable to know the real rheological properties of the ice, which usually are not described by a linear dependence between stress and strain.

COPYRIGHT: Arkticheskiy i antarkticheskiy nauchno-issledovatel'skiy institut (AANII), 1975

APPROVED FOR RELEASE: 2007/02/09: CIA-RDP82-00850R000500020040-0

APPROVED FOR RELEASE: 2007/02/09: CIA-RDP82-00850R000500020040-0

VIBRATIONS OF MEASUREMENT SYSTEMS IN A FLOW IN STUDIES OF OCEAN MICROSTRUCTURE

Leningrad TRUDY. ORDENA LENINA ARKTICHESKIY I ANTARKTICHESKIY NAUCHNO-ISSLEDOVATEL'-SKIY INSTITUT. RADIOFIZICHESKIYE METODY ISSLEDOVANIY VODNYKH MASS SNEGA I L'DA in Russian No 324, 1974 pp 126-133

[Article by A. V. Gusev and A. P. Polyakov]

[Text] In a study of microstructure of the sea medium measurements are made of its mean temperature, mean velocity, temperature fluctuations and fluctuations of flow velocity. Recently there has been a tendency to the use of low-inertia thermoanemometric sensors in measurements. These make it possible to register the change in the studied parameters with frequencies up to 20 Hz and amplitudes up to 0.05 mm/sec [1, 3]. However, thermistor-type sensors react to oscillatory motion and sometimes are used in registering the movements of measurement elements [2]. Therefore, the possible oscillations of the measurement system will be interference in the investigations. This article is devoted to the problems involved in the excitation of oscillations of some elements of measurement systems in flows and experimental investigation of these oscillations.

In studying the spatial characteristics of flow velocity and its pulsations it is customary to employ spatially separated systems of sensors. This spacing is accomplished by a distribution of the sensors along submerged electric or supporting cables or also on three-dimensional supporting frames of different configuration. The setting-out of these measurement systems is accomplished using supporting or electrical cables and bottom anchors and sunken floats in open seas and with lowering of the systems from the ice in arctic seas. The placement of the instruments at shallow depths is accomplished from the ice using rigid tubular rods.

In the presence of currents these submerged systems are all subjected to hydrodynamic pressures. With flow around any cylindrical body a dead space is formed in the flow behind it in which the water is at rest, that is, does not experience translational motion in the direction of the flow. In the boundary layer between the moving medium and the medium at rest shearing forces arise which are caused by viscosity of the medium. These forces give rise to a rotational movement in the medium at rest, leading to the formation of two symmetrically arranged nuclei of eddies which develop at the expense of one another due to a small initial asymmetry.

APPROVED FOR RELEASE: 2007/02/09: CIA-RDP82-00850R000500020040-0

APPROVED FOR RELEASE: 2007/02/09: CIA-RDP82-00850R000500020040-0

We will examine the eddy excitation of pulsations of different mechanical oscillatory systems. As a result of collapse of the eddies pressure impulses are created which act perpendicularly to the flow direction. In the eddy formation process there is formation of a periodic induced force capable of bringing the particular oscillatory system to its normal mode. At the present time, taking into account the role of eddy formation in the excitation of oscillations, it is assumed [5] that there is also a feedback, involving an influence of the oscillatory motion of the system on the process of formation and collapse of eddies. Thus, this phenomenon must not be regarded as an induced oscillation, but as an autooscillation. From this point of view excitation at the normal mode is completely understandable. A definite number of standing waves is induced in a flexible electrical or supporting cable. The frequency of the oscillations and the length of the oscillating segments of cable can be determined approximately using the Strouhal formula and the string equation respectively:

$$\mathrm{St} = \frac{f_s d}{V}; \quad l = \frac{1}{2f_0}\sqrt{\frac{T}{\mu_c}}, \tag{1}$$

where V is flow velocity; d is cable diameter; f_s is the eddy collapse frequency; T is cable tension; μ_c is linear density of the cable; f_0 is the frequency of characteristic oscillations; l is the length of a half-wave of oscillations.

The dimensionless Strouhal number St is dependent on the Reynolds number and is approximately 0.2 for Reynolds numbers $300 < R < 100\,000$. The frequency f_s is dependent on the flow velocity (linearly), the frequency of cable oscillations is dependent on the ratio of f_0 to f_s since the oscillations develop most intensively when there is an equality of these frequencies or at higher harmonics of oscillations of the system. Accordingly, the frequency of oscillations of the cable changes discretely from one form of oscillations to another; nevertheless, the mean frequency of the vibrations is almost linearly dependent on water velocity. When under the influence of static forces the cable slopes relative to the flow it is necessary to take its component in the direction perpendicular to the axis of the cable as the velocity determining the frequency of eddy collapse.

On the basis of expression (1), with small submergences of the systems and with small flow velocities it is possible to select such parameters of these systems with which there will be no excitation of vibrations. However, in actual practice this will not always be justified and in addition there are excitations of oscillations even in the case of laminar flow around bodies, that is, when the Reynolds number is less than 50. This suggests that in addition to the well-known mechanism of excitation of vibrations by the flow during eddy formation there is also another mechanism for the development of forces leading to the excitation of oscillations also in the case of small Reynolds numbers.

We will examine the behavior of a circular elastic cylinder in the flow. With a uniform movement of the cylinder in unbounded space of a nonviscous fluid the velocity at points on a cylinder is equal to [4]:

$$V = 2V_\infty \sin\Theta, \tag{2}$$

APPROVED FOR RELEASE: 2007/02/09: CIA-RDP82-00850R000500020040-0

APPROVED FOR RELEASE: 2007/02/09: CIA-RDP82-00850R000500020040-0

and the pressure distribution along the cylinder in the plane perpendicular to the axis is determined by the pressure coefficient

$$\bar{p} = 1 - \left(\frac{V}{V_\infty}\right)^2 = 1 - 4\sin^2\Theta. \tag{3}$$

For the lower half of the cylinder the V and $\bar{p}$ values are identical at points symmetric relative to x and y. Accordingly, the projection of the hydrodynamic reaction onto the x-axis (direction of movement) R_x, called drag, and also the projection onto the direction R_y perpendicular to movement, called lift, are identically equal to zero, which under real conditions is not observed. The reason for the development of the forces acting on the cylinder from the direction of the flow must be sought in the rejection of assumptions that the fluid is unbounded, that it is nonviscous and that there is a constancy of velocity.

We will examine the circulatory flow around a circular cylinder. We will superpose on noncirculatory flow around a cylinder a circulatory flow with a singularity (center of eddy) at the center of the cylinder. The characteristic function of this complex flow is expressed by the formula

$$W = V_\infty\left(z + \frac{r_0^2}{z}\right) + \frac{\Gamma}{2\pi i}\ln z, \tag{4}$$

where $\Gamma = \oint \bar{V}\, d\bar{r}$ is the velocity circulation; $z = x + iy$; r_0 is the cylinder radius.

Assuming that the velocity of the circulatory flow V in polar coordinates at any point of the fluid is equal to $\Gamma/2\pi r$ [4], we obtain the velocity at the cylinder surface in the form of the sum of the velocity of flow around a cylinder without circulation and the velocity of the circulatory flow

$$V_\Theta = V_{\Theta 1} + V_{\Theta 2} = 2V_\infty \sin\Theta + \frac{\Gamma}{2\pi r_0}. \tag{5}$$

The critical points on the cylinder K_1, K_2 are found under the condition $V_\Theta = 0$; then

$$\sin\Theta_K = -\frac{\Gamma}{2\pi r_0 V_\infty}. \tag{6}$$

Depending on the magnitude of the circulation there can be different variants of positioning of the critical points:

$\Gamma > 4\pi r_0 V_\infty$ -- the equation has no solution;
$\Gamma = 4\pi r_0 V_\infty$ -- the critical points merge into one;
$\Gamma < 4\pi r_0 V_\infty$ -- the critical points are symmetric relative to the x-axis.

For the latter case, using formula (5), we find that the velocity at points on the upper part of the cylinder $0 < \Theta < \pi$ is equal to

$$V_\Theta = -2V_\infty \sin\Theta + \frac{\Gamma}{2\pi r_0}, \tag{7}$$

APPROVED FOR RELEASE: 2007/02/09: CIA-RDP82-00850R000500020040-0

APPROVED FOR RELEASE: 2007/02/09: CIA-RDP82-00850R000500020040-0

and at points on the lower part of the cylinder $\pi \leqslant \theta \leqslant 2\pi$

$$V_n = +|2V_\infty \sin\theta| + \frac{\Gamma}{2\pi r_0}. \tag{8}$$

Using the Euler integral [4]

[In all cases B = upper; H = lower] $$p_n|_{-\frac{\rho V_n^2}{2}} = -p_n|_{+\frac{\rho V_n^2}{2}}, \tag{9}$$

we find that $p_{lower} < p_{upper}$, that is, pressure at symmetric points on the lower part of the cylinder is less than on the upper part. These pressures, summed over the surface of the cylinder, lead to the appearance of lift R_y which will be equal to

$$R_y = -\rho l \Gamma V_\infty, \tag{10}$$

where I is the generatrix of a cylinder of a unit height.

Accordingly, on any rotating cylinder with its relative movement in the fluid there will be a lift force operative which is proportional to the density of the fluid, velocity of the oncoming flow and circulation. The intensity of this force is proportional to the diameter of the cylinder. Under its influence the relative velocity of the body will experience changes in time with respect to both value and direction, that is, $\overline{V} = V(x,y,z,t)$. Problems related to unsteady movement of bodies in a fluid can be considered only in a case when the coordinate system moves together with the body. Solving these problems [4], we obtain an expression for drag in general form

[тр = app(arenc)] $$R_x = -m_{ap} \frac{dV}{dt}, \tag{11}$$

where m_{app} is the apparent mass of fluid.

The lift will displace the cylinder from a state of equilibrium and with the striving of the cylinder to occupy the most stable position there can be development of periodic oscillations in the direction across the flow. As a simplification we will assume that the oscillations are sinusoidal, that is, the velocity is equal to $V_y \sin\omega t$. Then the total velocity of the cylinder V will be

$$V = V_x + V_y \sin\omega t.$$

The expression for acceleration includes the term $\sin 2\omega t$, that is, the force acting on the body in the direction along the flow will be periodic and its frequency will exceed by a factor of 2 the frequency of the possible transverse oscillations.

With the submergence of the measurement systems from the surface weights are suspended to them; when they are installed on the bottom there are floats for ensuring tension of the cable and maintaining it in a vertical position, and also for decreasing the tilts of the instrument in the presence of currents. Depending on the relationship of the tensile stresses and weight of the electrical or supporting cable the systems will have different vibrational properties. If the tensile stress due to the weight or buoyancy greatly exceeds the weight of the cable the system

APPROVED FOR RELEASE: 2007/02/09: CIA-RDP82-00850R000500020040-0

APPROVED FOR RELEASE: 2007/02/09: CIA-RDP82-00850R000500020040-0

will be similar in its oscillation parameters to a string and the expression for the possible oscillations of the system with its displacement from a state of equilibrium has the form

$$y = A \sin \frac{n\pi}{l} x, \tag{12}$$

where A are arbitrary constants, determined from the boundary conditions; l is the length of the suspension.

As a simplification we will examine the oscillations in only one plane. The origin of coordinates is matched with the end of the suspension and the x-axis is directed along the line of the "fiber." With a predominance of the weight of the cable over the weight of the weight the system oscillations are similar to the oscillations of a fiber with a distributed weight and are determined by the expression

$$y = Ae^{i\omega t} I_0\left(2\omega \sqrt{\frac{x}{g}}\right), \tag{13}$$

where I_0 is a Bessel function of the first kind of a zero order; g is the acceleration of free falling.

An analysis of expressions (12) and (13) shows that a system similar to a string in an ideal case at its end does not have movements along the y-axis. However, a fiber with a distributed weight always has at its end a maximum amplitude of the displacements along the y-axis which is transmitted to the measuring instruments attached to the electrical or supporting cable at this place.

It follows from this analysis that in order to reduce the vibrations in the measurement systems in the flow it is necessary to decrease the diameters of the extended cylindrical elements of the systems, damp the rotational motion of these elements, strive to impart to the suspension system the vibrational properties of the string and ensure the independent collapse of the eddies along the extended elements of the system.

The experimental investigations of the vibrations of submerged systems arising in a flow were made using three-component vibrosensors. A vibrosensor was placed at the end of the submerged system in such a way that the response to vibrations in the vertical direction was 0.4 B/g, in two mutually perpendicular directions in the horizontal plane -- 1.8 B/g. A stabilizer is placed on the housing of the vibrosensor in order to ensure its orientation relative to the direction of flow.

The results of the experimental investigations confirmed that the vibration in the direction perpendicular to the direction of flow is most intense. It exceeds the longitudinal and vertical oscillations by an order of magnitude. Figure 1 shows the spectral characteristics of the oscillatory velocity in the transverse, longitudinal and vertical directions of the end of a cable with a diameter of 14 mm and a length of 20 m with a spherical weight at the end of 15 kg with a velocity of flow 7 cm/sec. The dashed sloping lines represent levels of equal displacements A. The values of the displacements and oscillatory velocity in Fig. 1 are given in real values, but for obtaining their amplitude values it is necessary that they be multiplied by 1.41.

APPROVED FOR RELEASE: 2007/02/09: CIA-RDP82-00850R000500020040-0

APPROVED FOR RELEASE: 2007/02/09: CIA-RDP82-00850R000500020040-0

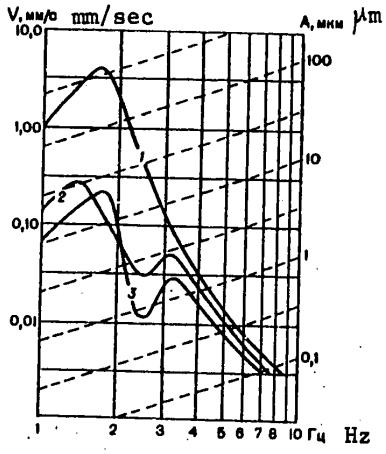

Fig. 1. Spectral characteristics A of oscillatory velocity V of end of cable in transverse (1), longitudinal (2) and vertical (3) directions.

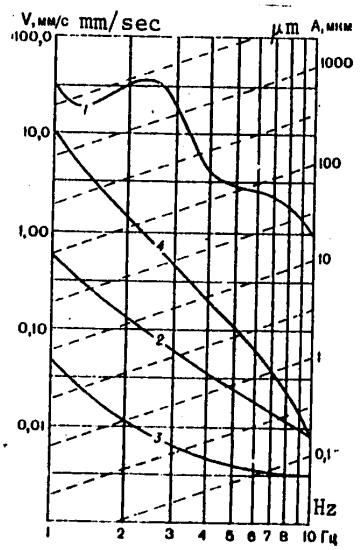

Fig. 2. Spectral densities A of oscillatory velocity V of different suspension systems. 1, 2, 3 -- oscillations of ends of 20-m suspensions (1 -- vibrosensor hung on 3-mm cable to which another 6-mm cable is attached; 2 -- hydrological weight of 15 kg suspended to same cables; 3 -- teardrop-shaped weight of about 300 kg suspended to cables, with three porolon vanes with a width of 15 cm and a length of 2 m attached to suspension cable; 4) oscillations of end of rigid rod formed by tubes with a diameter of 6 cm and a length of 15 m.

APPROVED FOR RELEASE: 2007/02/09: CIA-RDP82-00850R000500020040-0

APPROVED FOR RELEASE: 2007/02/09: CIA-RDP82-00850R000500020040-0

The oscillatory velocity of transverse vibrations in this case considerably exceeds the longitudinal and vertical oscillations. Since the longitudinal and vertical oscillations are a result of transverse oscillations, whose intensity considerably predominates, in the study of vibrations of submerged systems it is only necessary to register the latter. This made it possible, in a study of oscillations, to use thereafter a sensor in the form of a ceramic transducer having a spherical configuration and an identical response to vibrations in all directions, which does not require its orientation in the flow.

Although the most intense oscillations are excited with an equality of f_0 and f_s, with an increase in flow velocity there is a tendency to a linear increase in the frequency of the excited oscillations. Figure 2 shows the spectral densities of the oscillatory velocity of different suspension systems with a flow velocity of 10 cm/sec. A comparison of the oscillatory velocities of different systems shows that at some frequencies they differ by more than a factor of 1000. It is confirmed that a system similar to a string is more noise immune to vibrations than a fiber with a distributed weight.

Stabilizers with a weight and vanes on a cable impede the development of torsional oscillations of the system and vibrations, and also damp the system oscillations appearing due to eddy collapse.

The results of the experimental data also confirm that with an increase in the diameter of the cables there is an increase in the intensity of the oscillations (see Figures 1 and 2). Accordingly, even with relatively small current velocities the oscillatory velocity of individual parts of the suspension systems can attain large values (tens of millimeters per second). It is entirely natural that with the use of sensors reacting to oscillatory motion the hydrodynamic vibrations of the suspension systems will create high noise levels which limit the range of measurement of the registered values and in the absence of control can be erroneously considered to be the studied process.

Thus, on the basis of a theoretical analysis and experimental data the following was established:

1. During the study of the microstructure of the sea medium by sensors submerged on cables and rigid rods when currents are present there can be hydromechanical vibrations of the submerged system which are detectable by sensors responsive to movement.

2. If special measures are not taken for the damping of oscillations, the oscillatory velocities can attain tens of millimeters per second even with relatively low current velocities (up to 10 cm/sec).

3. When making such measurements it is necessary to monitor the oscillations of the suspension system by vibrodetectors at the places where sensors are attached.

4. In order to ensure the maximum noise immunity of submerged systems to vibrations an effort must be made to exclude rotations of elements of the system about its axis, decrease the diameters of the cables, have independent cutoff of the eddies

APPROVED FOR RELEASE: 2007/02/09: CIA-RDP82-00850R000500020040-0

APPROVED FOR RELEASE: 2007/02/09: CIA-RDP82-00850R000500020040-0

along the length of extended elements of the system (such as electrical and supporting cables), and also create a means for damping of the developing oscillations.

BIBLIOGRAPHY

1. Kiselev, V. P., "Apparatus and Method for Remote Measurements of the Statistical Characteristics of the Parameters of the Sea Medium and Waves," TRUDY AANII (Transactions of the Arctic and Antarctic Scientific Research Institute), Vol 284, pp 120-131, 1968.

2. Kiselev, V. P. and Naumenko, Yu. I., "Apparatus and Methods for Remote Monitoring of the Position and Stability of Underwater Measurement Systems," OKEANOLOGIYA (Oceanology), Vol VII, No 4, pp 691-696, 1967.

3. Kolesnikov, A. G. (et al.), "Experimental Investigations of Entrainment Under a Drifting Floe," FIZIKA ATMOSFERY I OKEANA (Physics of the Atmosphere and Ocean), Vol 1, No 12, pp 1310-1316 [year not given].

4. Fedyayevskiy, K. K. (et al.), GIDROMEKHANIKA (Hydromechanics), Leningrad, Sudostroyeniye, 1968, 421 pages.

5. Kharkevich, A. A., AVTOKOLEBANIYA (Autooscillations), Moscow, "Nauka," 1953, 93 pages.

COPYRIGHT: Arkticheskiy i antarkticheskiy nauchno-issledovatel'skiy institut (AANII), 1975

APPROVED FOR RELEASE: 2007/02/09: CIA-RDP82-00850R000500020040-0

APPROVED FOR RELEASE: 2007/02/09: CIA-RDP82-00850R000500020040-0

EXPERIENCE IN USING IR SCANNING APPARATUS ON THE SIXTEENTH SOVIET ANTARCTIC EXPEDITION (MARINE DETACHMENT)

Leningrad TRUDY. ORDENA LENINA ARKTICHESKIY I ANTARKTICHESKIY NAUCHNO-ISSLEDOVATEL'-SKIY INSTITUT. RADIOFIZICHESKIYE METODY ISSLEDOVANIY VODNYKH MASS SNEGA I L'DA in Russian No 324, 1974 pp 144-147

[Article by A. I. Galkina, Ye. A. Martynova, V. A. Spitsyn and A. M. Shalygin]

[Text] Remote thermal mapping on the basis of its characteristic infrared (IR) radiation is possible by employing IR apparatus situated on any moving carrier: aircraft, surface transport, ship, etc. It goes without saying in each specific case there will be definite peculiarities in the IR survey of a feature. It was of interest to study the possibility of using this apparatus on a ship because there is no information on the operation of IR scanning systems on ships. Earlier such IR apparatus successfully underwent aircraft tests in the Arctic, as a result of which a great mass of thermal data was obtained on the state of the sea surface covered with ice and concerning island glaciers [2].

An IR survey of the ocean surface was included in the work program of the radiophysics detachment of the scientific research ship "Professor Vize," which constituted part of the Sixteenth Soviet Antarctic Expedition. The laboratory was situated on the bridge deck on the ship's port side. The optical unit was set on a support attached to the deck and supplied with a rotating element which made it possible to select the optimum angle for scanning the investigated surface. Alongside the optical unit there was an aerial camera for the synchronous surveying of the examined surface. The scanning was carried out perpendicular to the direction of movement of the ship.

An IR survey of the ocean surface was made in the Strait of Magellan during the ship's run to Bellinsgauzen Station, and also in regions of floating ice and icebergs.

Figure 1,a shows a typical picture of the brightness contrasts of a sector of the water-ice surface. During operation the apparatus was adjusted in such a way that the colder sectors of the examined surface corresponded to a lighter tone of the photograph. Thus, water shows up as a dark background against which the ice can be seen in a gray-white tone. The presence of tone gradations is indicative of a different thickness of the ice. In general, the IR maps of the water-ice surface of the ocean obtained in work from the ship do not contain new information in comparison with the results obtained in the Kara Sea and are inferior to them in quality.

APPROVED FOR RELEASE: 2007/02/09: CIA-RDP82-00850R000500020040-0

APPROVED FOR RELEASE: 2007/02/09: CIA-RDP82-00850R000500020040-0

The setting up of the IR outfit optical unit at an angle to the scanned surface, rolling of the ship and nonuniformity of the rate of its movement cause appreciable distortions of the image.

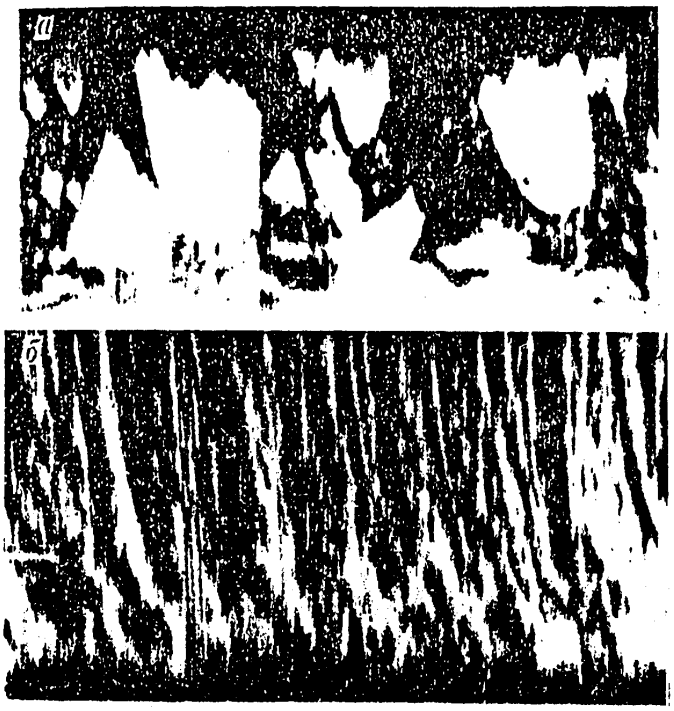

Fig. 1. IR map of sector of water-ice (a) and wave-covered (b) ocean surfaces.

A study was also made of the possibility of determining the state of the ocean surface using data from an IR survey. Figure 1,b shows an IR photograph of the wave-covered water surface. It is easy to see waves and the direction of movement of the waves, which confirms the assumption of the existence of brightness contrasts of the wave-covered ocean surface. The appearance of these contrasts when waves are present can be attributed, on the one hand, to temperature nonuniformity of the water surface as a result of intensive mixing. The lower limit of the temperature inhomogeneity, characterizing the thermal contrasts registered by the IR apparatus, is determined by the minimum temperature contrasts (ΔT_{min}) detectable by the IR apparatus. With a water temperature at the time of the survey 20°C $\Delta T_{min} = 0.06°$. On the other hand, when waves are present there is a change in the emission characteristics of the water surface, that is, the dependence of water emissivity on sighting angle is clearly expressed.

A negative result obtained in an attempt to determine the pattern of temperature contrasts of the thermal field of an iceberg is interesting. It was found that the IR scanning apparatus does not detect an iceberg against a sky background. The

APPROVED FOR RELEASE: 2007/02/09: CIA-RDP82-00850R000500020040-0

APPROVED FOR RELEASE: 2007/02/09: CIA-RDP82-00850R000500020040-0

iceberg was clearly visible on the photograph taken with an aerial camera. The IR map shows only the sky-ocean surface contrast and the iceberg cannot be distinguished. A reason for such a phenomenon can be postulated. As is well known, an object can be detected only in a case when its emission differs from the background emission. Since the IR radiation of an object is a function of its temperature and emissivity, it is obvious that the object and the background will be distinguished either under the condition of an inequality of their temperatures or with an identical temperature, but different emission coefficients. However, there can be such a combination of emissivities and temperatures of the object and its surroundings with which the radiation of the object is equal to the radiation of the background and there will be no brightness gradations on the photograph.

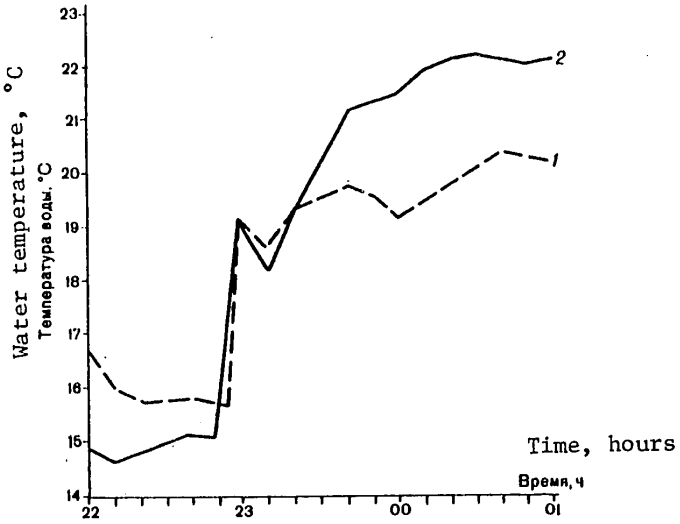

Fig. 2. Water temperature measured with a radiometer (1) and resistance thermometer (2) in convergence zone.

Due to malfunctioning of the apparatus it was not possible to obtain the pattern of thermal contrasts of the ocean surface in the convergence region. However, here the temperature of the water surface was measured with a radiation thermometer, which was also provided for by the work program of the radiophysical detachment. Earlier the radiation thermometer was used successfully in the Arctic [1,3]. Figure 2 shows the change in water temperature measured with a radiation thermometer and a resistance thermometer on a profile along the 20th meridian (in the convergence zone). In both cases the temperature jump moment is clearly expressed. The discrepancy in the readings of the thermometers is entirely understandable since the radiation thermometer measures the temperature of the water surface (the thickness of the layer forming the IR radiation in the range 8-12μm is several tens of micrometers) whereas the sensor of the resistance thermometer is at a depth of 5 m.

APPROVED FOR RELEASE: 2007/02/09: CIA-RDP82-00850R000500020040-0

APPROVED FOR RELEASE: 2007/02/09: CIA-RDP82-00850R000500020040-0

In conclusion it should be noted that the collected experimental data confirm the possibility of remote thermal mapping of the water-ice surface from aboard a ship. Despite some shortcomings, complicating the collection of qualitative thermal information under shipboard conditions, the IR apparatus on ships can be used in solving a number of problems in oceanology. We feel that it is possible to use these systems for studying the thermal structure of the water surface in zones of convergence (divergence), clusters of icebergs, currents and the coastal runoff of rivers both for the detection of these nonuniformities and for ascertaining the limits and extent of temperature anomalies. Evidently, such studies will require more detailed study of the possibilities of TV apparatus for investigation of thermal fields with a small temperature gradient, for example, in evaluating the degree of influence of disturbances of the characteristic radiation caused by waves on the detection of the thermal structure of the investigated objects.

BIBLIOGRAPHY

1. Galkina, A. I. and Spitsyn, V. A., "Measurement of Temperature of the Surface of Water, Snow and Ice With a Radiation Thermometer," TRUDY AANII (Transactions of the Arctic and Antarctic Scientific Research Institute), Vol 295, pp 61-68, 1970.

2. Martynova, Ye. A. and Spitsyn, V. A., "Some Results of Tests of a Scanning IR Apparatus for Obtaining Thermal Maps in Polar Regions," TRUDY AANII, Vol 295, pp 69-73, 1970.

3. Nalimov, Yu. V., "Use of a Radiation Thermometer in the Mouth Reaches of Siberian Rivers," PROBLEMY ARKTIKI I ANTARKTIKI (Problems of the Arctic and Antarctica), No 38, pp 129-132, 1971.

COPYRIGHT: Arkticheskiy i antarkticheskiy nauchno-issledovatel'skiy institut (AANII), 1975

APPROVED FOR RELEASE: 2007/02/09: CIA-RDP82-00850R000500020040-0

APPROVED FOR RELEASE: 2007/02/09: CIA-RDP82-00850R000500020040-0

THERMAL CONTRASTS OF A NATURAL WATER-ICE-SNOW SURFACE AND POSSIBILITY FOR QUANTITATIVE ESTIMATES OF SUCH CONTRASTS USING MEASUREMENTS BY IR METHODS

Leningrad TRUDY. ORDENA LENINA ARKTICHESKIY I ANTARKTICHESKIY NAUCHNO-ISSLEDOVATEL'-SKIY INSTITUT. RADIOFIZICHESKIYE METODY ISSLEDOVANIY VODNYKH MASS SNEGA I L'DA
in Russian No 324, 1974 pp 148-150

[Article by Ye. A. Martynova and V. A. Spitsyn]

[Text] An analysis of the results of an infrared (IR) survey of the water-ice sea surface [2] indicates that its thermal map includes information on the relationship of ice cover thicknesses. It is known that the distinguishability of objects on the thermal map is determined both by their temperature differential and by the different emissivity. If as a first approximation the emissivity of the investigated ice surface is considered homogeneous, the brightness contrasts on an IR photograph will be attributable to the temperature inhomogeneities of the ice surface. The difference in temperature of the ice surface, all other conditions being equal, will be dependent on the ice thickness and the relationship of air temperature and the heat influx from the water. Under natural conditions the ice is almost always covered with a layer of snow. The snow layer, a poor conductor of heat, on the ice surface will exert a screening influence on the detection of its temperature contrasts (and accordingly, also its changes in the ice thickness) and with certain definite thicknesses can completely distort the thermal pattern.

In the winter of 1973 work was carried out on Lake Ladoga for the purpose of detecting the possibility of remote estimation of the thickness of the snow cover on the ice (soil). Such an experiment is of interest for clarifying the screening influence of the snow on the ice surface on determination of the age stages of ice. In addition, the possibility of remote determination of the thickness of the snow cover is important for estimating the moisture reserve. The measurements were made in an area corresponding to the scanning strip of the IR scanning apparatus whose optical unit was situated at a height of 3 m from the investigated surface. The IR apparatus successively examined the surface of rocks, water, ice and snow cover (on the ice) of different thickness. The signal was registered by an amplitude indicator (S1-20 oscillograph). At the same time measurements were made of the temperature of the underlying surface by a contact method (MT-54 resistance thermometers cut into a bridge circuit). The signal was registered at different times of day under different meteorological conditions.

Figure 1 shows that change of the signal is easily traced in a successive examination of the snow cover on the ice, sectors of ice of different thickness and the surface of rock having a nonidentical temperature (and emissivity). The amplitudes

APPROVED FOR RELEASE: 2007/02/09: CIA-RDP82-00850R000500020040-0

APPROVED FOR RELEASE: 2007/02/09: CIA-RDP82-00850R000500020040-0

of signals from snow levels of different thickness lying on a homogeneous ice sector are clearly distinguishable. A signal from a snow layer of greater thickness, having a lower temperature, is stronger. A thin snow cover on ice with a thickness of 7 cm is perceived as warmer.

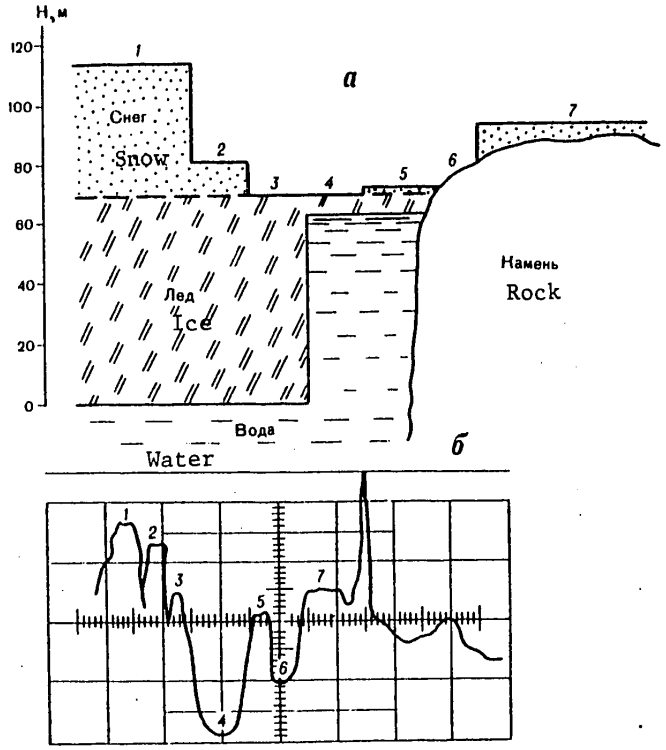

Fig. 1. One of variants of investigated surface (a) and corresponding signals on oscillograph screen (b).

In the course of the work we noted the following:

1. With a decrease in air temperature the registered thermal contrasts of the snow levels increase; this increase is especially conspicuous in the case of small Snow thicknesses. These results agree with the computational dependence obtained by Yu. P. Doronin for the relationship between temperature of the snow surface and air temperature and different thicknesses of snow and ice [1].

2. An increase in air temperature leads to a smoothing of the thermal contrasts of the snow cover. With air temperatures close to zero the snow levels were not distinguishable with the IR apparatus. On the other hand, with a decrease in positive air temperature (without passing through zero) the contrasts in thicknesses of the snow cover could be registered. An inversion was observed: in the IR survey the thicker snow layers were perceived as warmer.

APPROVED FOR RELEASE: 2007/02/09: CIA-RDP82-00850R000500020040-0

APPROVED FOR RELEASE: 2007/02/09: CIA-RDP82-00850R000500020040-0

3. The influence of solar radiation, which directly heats the snow cover surface and makes an IR contribution to the radiation detected by the IR apparatus, was substantial. The resulting pattern of thermal contrasts in this case is considerably distorted.

In addition to plotting of the thermal map by the scanning IR apparatus there was registry of the temperature of the investigated surface by use of a PRT-5 radiation thermometer (produced by the Barnes Engineering Company, United States). In a rock-snow level sector the radiation temperature for the rock was the principal source of information on the relationship of the thermal contrasts of the snow cover. This sector was at the boundary of the scanning strip of the IR apparatus and therefore the registered signal was distorted. As indicated by measurements with the PRT-5, the thermal contrasts of the snow levels on the rock and ice with similar thicknesses of the snow cover were not identical. The snow on the rock is perceived as being colder.

The collected experimental data make it possible to conclude that there is a possibility for remote determination of the thickness of the snow cover by the IR method, but in this process it is necessary to evaluate the limits of applicability of the method. Evidently, the distinguishability of snow sectors of different thickness will be determined by the thickness of the snow cover; by the relationship of air temperature and temperature of the surface underlying the snow cover at the time of measurements; by the preceding variation of temperatures; by the thermophysical characteristics of the snow. Computations with possible variants of the relationship of these factors are necessary.

BIBLIOGRAPHY

1. Doronin, Yu. P., TEPLOVOYE VZAIMODEYSTVIYE ATMOSFERY I GIDROSFERY (Thermal Interaction Between the Atmosphere and Hydrosphere), Leningrad, Gidrometeoizdat, 1969, 299 pages.

2. Martynova, Ye. A. and Spitsyn, V. A., "Some Results of Testing of IR Scanning Apparatus for Obtaining Thermal Maps in the Polar Regions," TRUDY AANII (Transactions of the Arctic and Antarctic Scientific Research Institute), Vol 295, pp 69-73, 1970.

COPYRIGHT: Arkticheskiy i antarkticheskiy nauchno-issledovatel'skiy institut (AANII), 1975

APPROVED FOR RELEASE: 2007/02/09: CIA-RDP82-00850R000500020040-0

APPROVED FOR RELEASE: 2007/02/09: CIA-RDP82-00850R000500020040-0

QUANTITATIVE ESTIMATE OF THERMAL RADIATION OF THE UNDERLYING SURFACE USING IR SCANNING APPARATUS

Leningrad TRUDY. ORDENA LENINA ARKTICHESKIY I ANTARKTICHESKIY NAUCHNO-ISSLEDOVATEL'-SKIY INSTITUT. RADIOFIZICHESKIYE METODY ISSLEDOVANIY VODNYKH MASS SNEGA I L'DA in Russian No 324, 1974 pp 197-203

[Article by Ye. A. Martynova and V. A. Spitsyn]

[Text] The principal characteristics of the IR scanning apparatus developed at the Arctic and Antarctic Scientific Research Institute and the possibilities of its use for thermal mapping of snow-ice surfaces have already been examined in [2]. Being a system for transforming the received IR radiation into a visible image, such an apparatus in principle makes it possible to measure the temperature of the investigated features. It is possible to realize the possibility of simultaneous registry of temperature of the underlying surface and its thermal mapping by introducing a special standard source whose radiation is compared with the radiation of the investigated object. From this point of view the optical system of the IR apparatus used earlier in experiments in the field of thermal mapping is optimum because it makes it possible to locate the source of reference (standard) radiation in such a way that the IR radiation of the investigated objects and the standard source travel one and the same optical path.

As the sources of a standard level of radiation necessary for a changeover to measurements of the temperatures of the investigated surfaces it is possible to use models of an ideally black body (IBB) built into the optical unit or other methods for obtaining a reference signal (for example, a method using the characteristic thermal radiation of the cooled detectors of IR radiation). The possibility of using a cooled radiation detector as the reference source is determined by the fact that the sensing element is at a constant temperature (in this case this is the boiling point of liquid nitrogen).

Now we will examine in greater detail the features of the IR apparatus reception unit and methods for its calibration.

The oscillogram (Fig. 1,a) makes it possible to determine the output voltages, proportional to the following difference fluxes, which act on the IR radiation detector:

APPROVED FOR RELEASE: 2007/02/09: CIA-RDP82-00850R000500020040-0

APPROVED FOR RELEASE: 2007/02/09: CIA-RDP82-00850R000500020040-0

$$\Delta\Phi_1 = \Phi_{IBB_1} - \Phi_{det}; \quad (1)$$

$$\Delta\Phi_2 = \Phi_{IBB_1} - \Phi_{surf}; \quad (2)$$

$$\Delta\Phi_3 = \Phi_{IBB_1} - \Phi_{IBB_2}; \quad (3)$$

$$\Delta\Phi_4 = \Phi_{IBB_2} - \Phi_{surf}; \quad (4)$$

$$\Delta\Phi_5 = \Phi_{IBB_2} - \Phi_{det}; \quad (5)$$

$$\Delta\Phi_6 = \Phi_{surf} - \Phi_{det}, \quad (6)$$

where Φ_{IBB} is the flux from the corresponding IBB model; Φ_{surf}, Φ_{det} are the fluxes from the investigated surface and the detector of IR radiation.

It therefore follows that with a known emissivity the temperature of the investigated surface can be determined by interpolation or extrapolation methods in a case when in the field of view of the optical system there are two standard radiation sources (for example, 1 and 2 in Fig. 1,b), whose temperature is different and can be measured.

However, the nonlinearity of the dependence between temperature and the radiation flux, especially in the range of low temperatures, leads to substantial errors in determining temperature.

Better results can be obtained if one of the following calibration curves is first obtained:

$$T_{surf} = f(\Delta\Phi_2) \text{ with } T_{IBB_1} = \text{const}; \quad (7)$$

$$T_{surf} = f(\Delta\Phi_4) \text{ with } T_{IBB_2} = \text{const}; \quad (8)$$

$$T_{surf} = f(\Delta\Phi_6) \text{ with } T_{det} = \text{const}. \quad (9)$$

In the first two cases the radiation of the IBB models is the reference radiation; in the third the reference level is provided by the characteristic radiation of the IR radiation detector (autocollimation case).

It is of interest to determine the most acceptable variant of calibration for the IR apparatus.

If expressions (2), (4), (6) are written in greater detail, in each case taking into account the position of the scanning mirror (see Fig. 1), after corresponding transformations it is possible to obtain the following expressions characterizing the difference fluxes operative on the detector of IR radiation (Φ_2; Φ_4; Φ_6):

$$\Delta\Phi_2 = \Phi_{IBB_1} + (1 - \varepsilon_{IBB})(\Phi_{opt} + \Phi_{det}) - (1 - \varepsilon_{det}) \quad IBB_1 - \Phi_{surf} - (1 - \varepsilon_{surf})$$
$$(\Phi_{opt} + \Phi_{det}) + (1 - \varepsilon_{det})\Phi_{surf}; \quad (10)$$

APPROVED FOR RELEASE: 2007/02/09: CIA-RDP82-00850R000500020040-0

APPROVED FOR RELEASE: 2007/02/09: CIA-RDP82-00850R000500020040-0

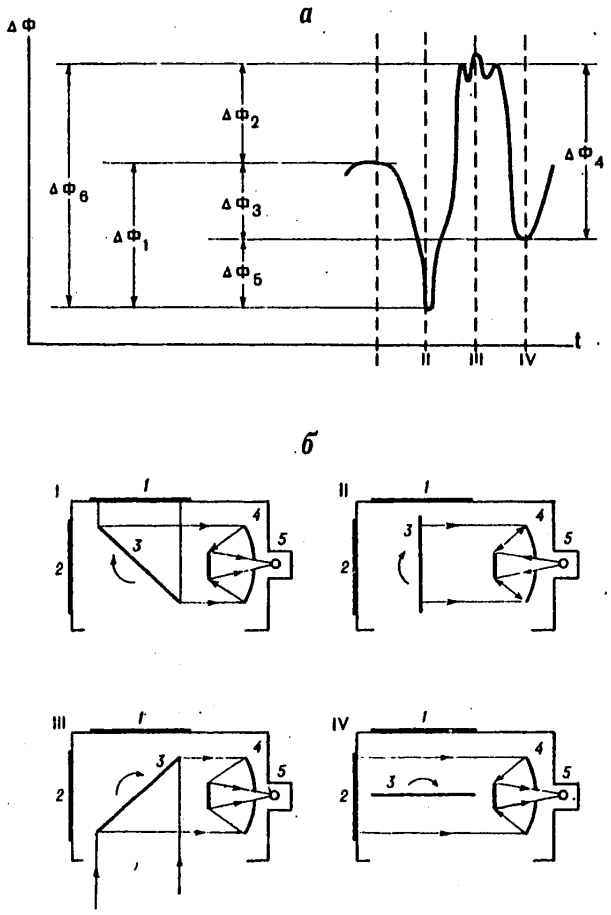

Fig. 1. Shape of output signal on screen of amplitude indicator (a) and diagram of optical unit for moments in time corresponding to different positions of scanning mirror I, II, III, IV (b). 1, 2) IBB models; 3) scanning mirror; 4) objective; 5) detector of IR radiation. I) radiation of IBB_1 is received; II) detector "looks" at itself (autocollimation); III) the investigated surface is examined; IV) the radiation of IBB_2 is incident directly on detector.

Table 1

Temperature of optical parts, °C	$\Delta\Phi_2$	$\Delta\Phi_4$	$\Delta\Phi_6$
		W·10⁻⁷	
-9	1.2684	0.9190	0.7161
-1	1.2670	0.8974	0.6982

APPROVED FOR RELEASE: 2007/02/09: CIA-RDP82-00850R000500020040-0

APPROVED FOR RELEASE: 2007/02/09: CIA-RDP82-00850R000500020040-0

$$\Delta\Phi_4 = \Phi_{IBB_2} + (1 - \varepsilon_{IBB})(\Phi_{det} + \Phi_{ob}) + \Phi_{ob} - (1 - \varepsilon_{det})(\Phi_{ob} + \Phi_{IBB_2}) - \Phi_{surf} - (1 - \varepsilon_{surf})(\Phi_{det} + \Phi_{opt}) - \Phi_{opt} + (1 - \varepsilon_{det})(\Phi_{surf} + \Phi_{opt}); \quad (11)$$

$$\Delta\Phi_6 = \Phi_{surf} + (1 - \varepsilon_{surf})(\Phi_{det} + \Phi_{opt}) - (1 - \varepsilon_{det})\Phi_{surf} - (1 - \varepsilon_{opt})(\Phi_{det} + \Phi_{ob}); \quad (12)$$

where Φ_{opt}, Φ_{ob} are the radiation fluxes of the optical parts and objective respectively; ε_{IBB}, ε_{opt}, ε_{det}, ε_{surf} are radiation coefficients.

Using the expressions for the difference fluxes (10)-(12) and the tables published by M. A. Bramson [1], the authors made computations for the purpose of determining the influence of changes in temperature of the optical elements of the IR apparatus on the difference flux as a function of the calibration method. The initial data for the computations are given below:

Radiating object	IBB_1	IBB_2	IR radiation detector	Optical parts	Investigated surface
Temperature of object, °C	9	5	-33	-9, -1	-13

The results of the computations are given in Table 1. The cited data show that the difference fluxes, and accordingly the registered signal, are dependent on the temperature of the optical parts of the IR apparatus receiving unit. It can be noted that the minimum influence is exerted by a change in the temperature of the optical system on the signal caused by the resultant flux

$$\Delta\Phi_2 = \Phi_{IBB_1} - \Phi_{surf}.$$

The difference fluxes $\Delta\Phi_4$ and $\Delta\Phi_6$ corresponding to the use of IBB_2 and a detector of their radiation (autocollimation method) as a measurement standard are approximately identically subject to the influence of temperature instability of the optical parts.

Accordingly, from the point of view of the nondependence of the registered signal on the temperature of the optical parts of the IR apparatus it is preferable to use in calibration the radiation of a model of an ideally black body IBB_1.

Now we will discuss the calibration method and method for subsequent temperature measurements of the investigated surface. Taking the above recommendations into account, our IR apparatus, which for the most part was intended for making observations from an aircraft, was supplied with a built-in IBB model situated in front of the input element of the optical unit -- a scanning plane-parallel mirror. The positioning of the standard source corresponds to the position of IBB_1 in Fig. 1. Due to the considerable size of the objective used in the optical unit, constructed in a Cassegrainian scheme (diameter of entrance aperture 150 mm), it is necessary to use a model of an IBB with a large area of the entrance window. This condition follows from the basic requirement on the design of the optical channel, in which it is necessary to ensure a nondependence of the radiant flux at the input of the IR radiation detector on the distance to the investigated surface [3].

APPROVED FOR RELEASE: 2007/02/09: CIA-RDP82-00850R000500020040-0

APPROVED FOR RELEASE: 2007/02/09: CIA-RDP82-00850R000500020040-0

In other words, the IBB model must be an extended source whose surface always overlaps the optical channel field of view.

The large size of the IBB model in turn complicates the temperature stabilization process. The accuracy in maintaining this temperature at a stipulated level determines the accuracy in measuring the temperature of the investigated objects. The difficulties are also aggravated by the fact that in the design of the used optical unit the "IR apparatus" is not protected from the atmospheric effects of the entrance window. The absence of the protected entrance window, however, in combination with a strongly ventilating rotating plane-parallel mirror, does not make it possible to ensure an acceptable accuracy in maintaining the temperature of the standard source during flights under changing climatic conditions. Accordingly, it is desirable to desist completely from temperature stabilization of the used IBB model. In this case the temperature of the investigated surfaces can be determined in the following way: making use of temperature sensors, in the course of measurements there is constant registry of the temperature of the IBB model, whereas the temperature of the investigated surface is ascertained from an earlier plotted calibration curve corresponding to the range of temperature changes of the IBB model (under measurement conditions) and the output signal value.

Using this method plans call for obtaining a family of calibration curves whose parameter is T_{IBB},

$$T_{surf} = f(\Delta\Phi) = f(K\Delta U), \tag{13}$$

where T_{surf} is surface temperature; $\Delta\Phi$ is the registered difference of fluxes; U is the output voltage; K is a proportionality factor.

Despite the fact that this calibration method seems simple, it is inconvenient due to considerable expenditures of working time, also related to the need for obtaining individual calibration curves for surfaces with different emissivity.

Therefore, when it is impossible to use the method for stabilization of a standard source, for the calibration of a scanning IR apparatus it is proposed that use be made of a simpler method in which two "extended" standard sources (IBB models), identical in their characteristics, must be used. One of these is built in to the optical unit like the IBB_1 (see Fig. 1), whereas the other (IBB_3) simulates the radiation of the investigated surface.

In this case it is possible, quite simply, to obtain a single standardized calibration curve

$$T_{IBB} = f(\Delta\Phi) = f(KU). \tag{14}$$

In order to determine this dependence the output voltage value is read from the amplitude recorder screen. This voltage corresponds to the difference in the radiation fluxes of the used IBB models with a different IBB temperature simulating the underlying surface. The IBB temperature of the IR apparatus installed in the optical unit is maintained during calibration of the constant.

Figure 2 shows a variant of the calibration curve of the dependence of the output voltage U_{out} of the IR apparatus on IBB temperature.

APPROVED FOR RELEASE: 2007/02/09: CIA-RDP82-00850R000500020040-0

APPROVED FOR RELEASE: 2007/02/09: CIA-RDP82-00850R000500020040-0

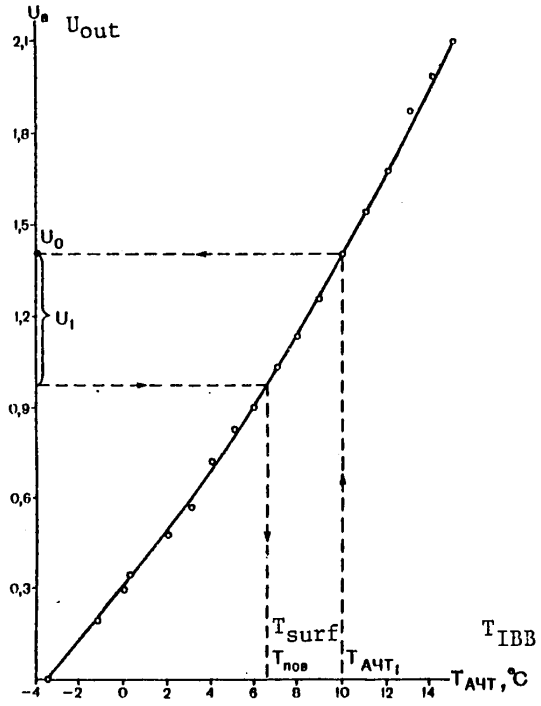

Fig. 2. Variant of calibration curve.

Under natural conditions, when a thermal survey is made from an aircraft, the radiation temperature of the investigated object can be determined from the known temperature of the IBB built into the optical unit and the amplitude of the signal registered on the oscillogram corresponding to the difference in the IBB - investigated object fluxes: using the calibration curve we find the U_0 value corresponding to a particular IBB temperature (see Fig. 2). Then, knowing that the temperature of the investigated surface is higher or lower than the IBB temperature (this can be seen on the amplitude indicator screen), we ascertain from the U_0 value the amplitude of the signal U_1 and using the calibration curve we determine the sought-for temperature of the object T_1.

It should be emphasized that the condition of constancy of IBB_1 temperature is not necessary; it is only sufficient to know its value at the time of measurement of temperature of the investigated object.

It is entirely understandable that by using the constructed calibration curve under the real conditions of an IR survey it is possible to ascertain the radiation temperature of the investigated object. However, conversion to thermodynamic temperature is possible if the emissivity coefficient is known for a given temperature and the spectral range employed.

APPROVED FOR RELEASE: 2007/02/09: CIA-RDP82-00850R000500020040-0

APPROVED FOR RELEASE: 2007/02/09: CIA-RDP82-00850R000500020040-0

BIBLIOGRAPHY

1. Bramson, M. A., SPRAVOCHNYYE TABLITSY PO INFRAKRASNOMU IZLUCHENIYU NAGRETYKH TEL (Reference Tables for IR Radiation of Heated Bodies), Moscow, "Nauka," 1965, 320 pages.

2. Martynova, Ye. A. and Spitsyn, V. A., "Some Results of Tests of a Scanning IR Apparatus for Obtaining Thermal Maps in the Polar Regions," TRUDY AANII (Transactions of the Arctic and Antarctic Scientific Research Institute), Vol 235, pp 69-73, 1970.

3. Nikolayev, S. M., OPTIKO-ELEKTRONNYYE RADIOMETRY KOSMICHESKIKH APPARATOV (Optical-Electronic Radiometers of Space Vehicles), Moscow, "Mashinostroyeniye," 1971, 178 pages.

COPYRIGHT: Arkticheskiy i antarkticheskiy nauchno-issledovatel'skiy institut (AANII), 1975

- END -

5303
CSO: 8144/0318

APPROVED FOR RELEASE: 2007/02/09: CIA-RDP82-00850R000500020040-0